LAPPEENRANTA UNIVERSITY OF TECHNOLOGY
LUT School of Energy Systems
LUT Mechanical Engineering

Jussi Kinnunen

CONTROLLING FULL PENETRATION IN MAG WELDING BY THE APPLICATION OF INFRARED THERMOGRAPHY AND NEURAL NETWORK

Examiners: Prof. Jukka Martikainen
Lic.Sc. (Tech) Miikka Karhu

ABSTRACT

Lappeenranta University of Technology
LUT School of Energy Systems
LUT Mechanical Engineering

Jussi Kinnunen

CONTROLLING FULL PENETRATION IN MAG WELDING BY THE APPLICATION OF INFRARED THERMOGRAPHY AND NEURAL NETWORK

Master's thesis

2016

67 pages, 27 figures, 4 tables, and 2 appendices

Examiners: Prof. Jukka Martikainen
Lic.Sc. (Tech) Miikka Karhu

Advisor: M.Sc. Esa Hiltunen

Keywords: Adaptive welding, infrared thermography, neural network, MAG, GMAW

Various sensors and monitoring equipment, such as infrared sensors and laser scanners for sensing welding quality have recently become affordable. The most advanced application for these sensors would be an adaptive, self-adjusting welding station. Equipment manufacturers have successfully developed systems for online quality monitoring commonly used in for example continuous pipe manufacturing. However there is still no perfectly developed and completely adaptive welding software available. The benefits of adaptive welding would be increased quality due to automatic correction when welding conditions change and decreased fabricating time and cost as, for example, weld backing supports would be replaced with an adaptive weld penetration control.

In this study, an infrared thermography based sensor was studied with regard to usability and the accuracy of sensor data as a weld penetration signal in gas metal arc welding. The object of the study was to evaluate a specific sensor type which measures thermography from solidified weld surface. The purpose of the study was to provide expert data for developing a sensor system in adaptive metal active gas (MAG) welding. Welding experiments with considered process variables and recorded thermal profiles were saved to a database for further analysis. To perform the analysis within a reasonable amount of experiments, the process parameter variables were gradually altered by at least 10 %. Later, the effects of process variables on weld penetration and thermography itself were considered. SFS-EN ISO 5817 standard (2014) was applied for classifying the quality of the experiments. As a final step, a neural network was taught based on the experiments. The experiments show that the studied thermography sensor and the neural network can be used for controlling full penetration though they have minor limitations, which are presented in results and discussion. The results are consistent with previous studies and experiments found in the literature.

TIIVISTELMÄ

Lappeenrannan teknillinen yliopisto
LUT School of Energy Systems
LUT Kone

Jussi Kinnunen

LÄPIHITSAUTUVUUDEN VARMISTAMINEN MAG-HITSAUKSESSA INFRAPUNA-TERMOGRAFIAN JA NEUROVERKON AVULLA

Diplomityö

2016

67 sivua, 27 kuvaa, 4 taulukkoa ja 2 liitettä

Tarkastajat: Prof. Jukka Martikainen
TkL Miikka Karhu

Ohjaaja: DI Esa Hiltunen

Hakusanat: Adaptiivinen hitsaus, infrapuna-termografia, neuroverkko, MAG-hitsaus

Hitsauksen anturit ja monitorointijärjestelmät ovat kehittyneet viimeaikoina riittävän käyttökelpoisiksi ja edullisiksi hitsauksen laadunhallintaan. Kehittynein sovelluskohde kyseisille laitteille olisi itsesäätyvä hitsausjärjestelmä. Laitevalmistajat ovat kehittäneet järjestelmiä laadunvalvontaan esimerkiksi putkien hitsaamisessa jatkuvana prosessina, mutta kuitenkaan kaupallisia, täysin adaptiivisia järjestelmiä ei ole saatavilla. Adaptiivisen hitsauksen etuja ovat parantunut laatu hitsausparametrien automaattisen säädön ansiosta ja pienenevät kustannukset, kun esimerkiksi juurituet korvataan automaattisella läpihitsautuvuuden hallinnalla.

Tässä tutkimuksessa tarkasteltiin infrapuna-termografiaan perustuvan anturin käyttökelpoisuutta läpihitsautuvuuden hallinnassa. Tutkimuksen tarkoitus oli tuottaa asiantuntijadataa adaptiivisen itsesäätyvän hitsausjärjestelmän kehittämisen pilottihanketta varten. Kokeet suoritettiin päittäisliitoksena V-railotyypille robotisoidulla metallikaasukaarihitsauksella. Hitsauskokeiden muuttuvia hitsausparametreja varioitiin vähintään 10 % kerrallaan, jotta tulosten analysointi onnistui järkevällä koemäärällä. Kokeiden aikana hitsausparametrit ja termografiadata tallennettiin sähköisesti arviointia varten. Koehitsien laadun luokitteluun käytettiin SFS-EN ISO 5817 -standardia (2014). Hitsauskokeiden pohjalta opetettiin neuroverkko, jolla simuloitiin hitsausprosessin säätöä. Tutkimustuloksina havaittiin, että tutkittu infrapuna-termografia-anturi ja neuroverkko ovat käyttökelpoisia läpihitsautuvuuden anturoinnissa, vaikka myös rajoituksia, joista keskustellaan tuloksissa ja johtopäätöksissä, havaittiin. Tämän työn tutkimustulosten huomattiin olevan linjassa aiempien tieteellisten julkaisujen tulosten kanssa.

ACKNOLEDGEMENTS

This study was carried out as a part of the Adaptive welding project (Neural) funded by the Finnish Funding Agency for Innovation (TEKES) and Lappeenranta University of Technology (LUT). The author thanks all participants in the project for their contribution and especially for their support of this study.

I consider myself privileged being able to work with professionals of modern welding technology. I would like to thank examiners of my thesis Professor Jukka Martikainen and Lic.Sc. (Tech) Miikka Karhu for providing me this great opportunity for scientific research. I would also like to thank my advisor M.Sc. Esa Hiltunen for providing me with important comments and advice. Special thanks go to our soft computing specialist Dr.Sc. (Eng.) Juho Ratava as well as laboratory technicians Antti Kähkönen and Harri Rötkö for helping with the building of experimental setups.

I want to thank my family and friends for motivating and supporting me during my studies at the Lappeenranta University of Technology.

I would like to cite a good friend of mine: *"Before this study I knew nothing, however now I know everything"*.

Jussi Kinnunen
Lappeenranta
15th of May 2016

TABLE OF CONTENTS

LIST OF SYMBOLS AND ABBREVIATIONS

ε	Spectral emissivity coefficient	
λ	Wavelength	[m]
b	Root reinforcement width	[mm]
C_1	The first universal radiation constant	
C_2	The second universal radiation constant	
e	Euler‘s number	
E	Arc energy	[kJ/mm]
fps	Frames per second	
h	Root reinforcement height	[mm]
I	Spectral hemispherical emissive power	[W/m^2]
I^b	Spectral hemispherical emissive power of the black body	[W/m^2]
T	Temperature	[°C, K]
T_{max}	Maximum infrared temperature	[°C]
V	Travel speed	[mm/s]
W	Wire feed rate	[m/min]

AI	Artificial intelligence
Ar	Argon
CCD	Charge coupled device
CMOS	Complementary metal oxide semiconductor
CO_2	Carbon dioxide
CTWD	Contact tip to work distance
DCEN	Direct current, electrode negative
DCEP	Direct current, electrode positive
DOF	Degree of freedom
F&AWMT	Flexible and agile welding manufacturing technology
GMAW	Gas metal arc welding
IIW	International Institute of Welding
IR	Infrared
IRT	Infrared thermography

IRWT	Intelligent robot welding technology
IWM	Intelligent welding manufacturing
IWMT	Intelligent welding manufacturing technology
LWIR	Long wavelength infrared
MAG	Metal active gas welding
MIG	Metal inert gas arc welding
MSE	Mean squared error
MWIR	Middle wavelength infrared
NDT	Non-destructive testing
NIR	Near wavelength infrared
PI	Proportional-integral controller
PID	Proportional-integral-derivative controller
RMS	Root mean square
RMSE	Root mean squared error
TPS	ThermoProfilScanner
TIG	Tungsten inert gas welding
V&DWMT	Virtual and digital welding manufacturing technology

1 INTRODUCTION

The welding industry is one of the major players in maximal production automation. The motivation of production automation is to increase competitiveness by improving productivity, quality and cost efficiency. Robotic arc welding is currently the most common application of welding automation. With a share of more than 60 %, the automotive industry is currently the predominant user of robotics for various welding processes and material handling (Hägale, Nilsson & Pires, 2008, p. 963–964.) Thus, there are also several other products made by robotic welding. In addition, other mechanisation and automation solutions, for example welding tractors and manipulators, are also applied.

Welding processes tend to be complicated due to the huge amount of variables, requiring high accuracy, knowledge, and great skills. Modern automation equipment, such as welding robot is able to make better single welds than a human welder. However, robot welding systems have lacked one crucial skill that human welders have: adjusting to variations in welding conditions. Welding conditions are never exactly the same, therefore professional welders use their senses to produce the best possible weld quality. Even small faults on pre-machining the seam and heat distortion are likely to cause imperfections and decrease the welding quality, especially if the welding process is not adjusted to changing welding conditions. In addition, manually teaching a robot for every welding task is time-consuming and unproductive. That is why there has been a great need to develop welding robots that automatically adjust to variations in the welding conditions just like a talented professional welder does. (Hägale et al., 2008, p. 969–970; Chen & Lv, 2014, p. 109–110.)

Fully automatic, self-adjusting welding requires a reliable feedback quality control system. However, the progress in the field of development and research of modern welding technology has made self-adjusting, adaptive welding possible. Nowadays, this type of adaptive welding automation is technically possible also for demanding welding processes, such as gas metal arc welding, gas tungsten arc welding and laser welding, requiring accurate weld pool control. Various welding quality control approaches, such as infrared thermography sensors and neural network based welding control systems, have been studied and proposed. Though, there is still a lot of further development needed for developing

commercial adaptive welding control systems. (Chen et al., 2014, p. 109–110; Pires, Loureiro, & Bölmsjo, 2006, p. 1–5, 73.)

1.1 Background

Investments for state-of-art welding research have always been on the agenda of the Lappeenranta University of Technology. One of the latest projects is aiming to develop a prototype of a commercial adaptive welding system. This study is related to the development of a sensor monitoring system for the prototype adaptive welding system.

1.2 Objectives and limitations

The objective of this research was to evaluate the usability of an infrared thermography sensor and a neural network for monitoring full penetration in robotic gas metal active gas (MAG) welding. The purpose of this study was to provide information about the special features of infrared sensing for the development of an adaptive sensor monitoring system. This study focuses experimentally on a specific infrared sensor type and the welding experiments were performed only in a specific butt welding case.

Research questions of the study are:

1. What kind of state-of-art studies has been recently executed about adaptive welding technology and what is the general level of adaptive technology in the welding industry?
2. Can weld penetration be monitored by infrared thermography in adaptive MAG welding and what is the accuracy of the measurements?
3. What are the practical benefits and limitations of infrared thermography?
4. Can weld penetration be estimated by neural network based welding process modelling and studied infrared thermography sensor?
5. How should infrared thermography data be processed and linked for an adaptive control system?

1.3 Research methods

This study consists of two main sections: literature review and description of the experimental work. The literature review introduces the fundamentals of adaptive welding in chapter 2, modern arc welding sensors in chapter 3, welding process control strategies in

chapter 4 and recent state-of-art studies of adaptive welding as well as industrial cases in chapter 5. The purpose of the literature review is to gather scientific information from recent studies to support the analysis of the results of this study. The information presented in the literature review is based on scientific articles and textbooks. Reliability of the references is surveyed.

Welding experiments were performed using robotic gas metal arc welding. The varied parameters and variables used were travel speed, wire feed rate, arc length (voltage), root gap and root face. The analysis of the effects of the parameters or variables on the results of the study was made possible by comprehensive classification and varying the parameters in the experimental procedure at least 10 % at a time. Specimens for macroscopic examination and weld attribute evaluation by applying SFS-EN ISO 5817 standard (2014) were used for evaluating the full penetration in the experiments. Later, a neural network was taught and verified based on the classified experiments. The neural network was applied for simulating and testing penetration control by the infrared thermography sensor data.

1.4 Significance of the topic and used references

Reliability of used information was ensured by using scientifically valid articles, books and conference papers. The information was acquired from several scientific instances, such as Science Direct, Springer, Google Scholar and Scopus database. The validity of the information was ensured by using cross-referencing and by preferring peer reviewed articles. The terminology used in this thesis was based on SFS 3052 standard (1995). As well, Scopus was used for analysing the sources.

Scopus searches were executed using search term:

- “adaptive” AND “welding”
- “adaptive” OR “intelligent” OR “automated” AND “welding”
- “infrared thermography” AND “welding”
- “neural network” AND “welding”

The literature analysis using search terms “adaptive” OR “intelligent” OR “automated” AND “welding” resulted in 3922 documents found. At least 1328 documents were related to neural networks. However, only 195 documents were related to infrared thermography. Most of the

documents were produced in China, United States, Germany, United Kingdom and Japan. The distribution of documents by year is shown in figure 1. Most of the adaptive welding publications are written in 2000's and 2010's. The number of publications has increased significantly since 1970. It can also be detected that the 1980's was a significant period because sensor technology rapidly developed.

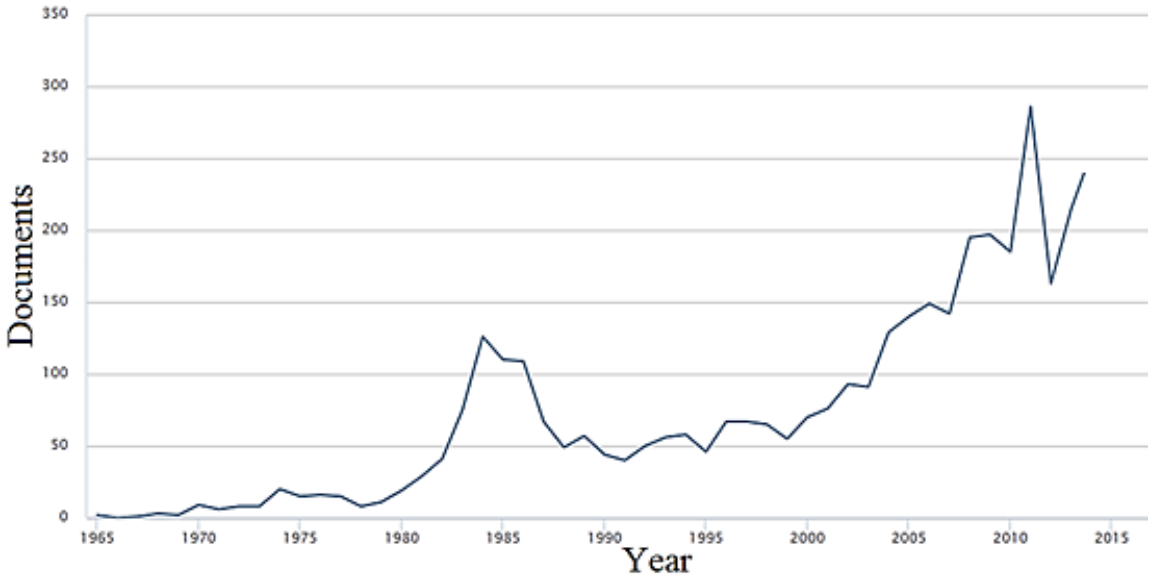

Figure 1. Documents published by year that include the search term "adaptive" OR "intelligent" OR "automated" AND "welding" (Scopus, 2016).

The specific types of documents published about adaptive welding are categorised in figure 2. The published documents are mostly articles and conference papers, although all other types are present as well.

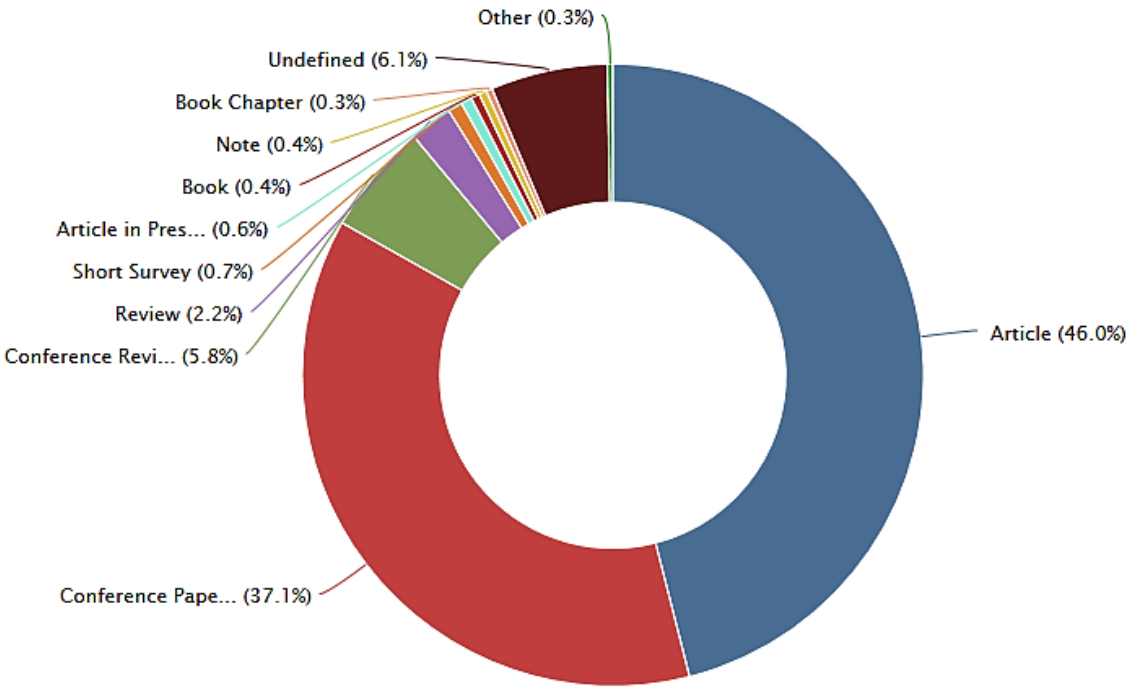

Figure 2. The types of documents published that include the search term “adaptive” OR “intelligent” OR “automated” AND “welding” (Scopus, 2016).

Adaptive welding and infrared thermography have been studied for a few decades, however there is still a lot of work to be done. Sensor signals play a significant role when developing an adaptive welding system. Since previous studies with similar infrared thermography sensor were not available, this experimental study was found necessary.

2 ADAPTIVE WELDING

Industrial robots are the dominant class of welding mechanisation equipment. Although robots are themselves efficient and flexible machines able to perform demanding welding tasks almost perfectly, there are several problems for exploiting the full benefits of the flexibility of these robots. In fact, applying a robot to a welding task will increase the complexity of the process because programming and maintaining robot systems require a high level of knowledge and skill from the operators. In addition, traditional teaching methods for path programming are time-consuming. That leads to a need to develop more efficient and easy to use robot-human user interfaces. (Pires et al., 2006, p. 17–23; Chen et al., 2014, p. 109–110.)

2.1 What does adaptive welding mean?

The terms “robotic welding” and “mechanised welding” themselves do not mean that the welding is done completely automatically. Most of the robots and manipulators used in the industry are still teach and playback based systems, requiring a weld path teaching for every welding situation. This class of welding systems does not represent a high level of automation, although they represent a good level of mechanisation. In general, fully automatic and self-adjusting welding has been referred to by the well-established term “adaptive welding” and sometimes with terms such as “intelligent welding” or “automatic welding”. The adaptive, high-end welding systems are equipped with software and systems that provide automatized features and more efficient productivity with higher duty cycle. Adaptive welding has to have at least some kind of quality based feedback signal. (Pires et al., 2006, p. 17–23; Heston, 2005, p. 41–44; Chen et al., 2014, p. 109–110.)

2.2 Benefits and possibilities of adaptive welding

The motivation of adaptive welding is to offer solutions to the needs of the industry, such as minimising costs, improving productivity and improving quality. Adaptivity is an important factor in welding automation. Adaptive welding tries to simulate experienced human welders’ logic of making decisions and performing welding. Without adaptivity, a robot is unable to automatically adjust to varying circumstances and perturbations, for example inaccuracies caused by machining, plate distortions and path teaching problems. Welding

also involves some dangerous factors, such as hot metal and unhealthy fumes, which can be solved by keeping the welding operator away from the welding process. However, the considered factors change when humans are replaced by robots. The most important features that make robots suitable for welding are: high accuracy and repeatability (better than 0.1 mm), good payload capacity, degrees of freedoms (usually 6 DOF), fast actuator speed and acceleration as well as comprehensive communication buses. (Pires et. al., 2006, 22–23; Chen et al., 2014, p. 117–119; Heston, 2005, p. 41–44.)

2.3 Levels of adaptive welding technology

According to Chen's review on intelligent welding manufacturing (IWM), adaptive welding technology, also known as intelligent welding manufacturing technology (IWMT) can be classified into various levels of technological fields of research. Intelligent welding technology consists of three fields of modern welding technology: the virtual and digital welding manufacturing technology (V&DWMT), the intelligent robot welding technology (IRWT) and the flexible and agile welding manufacturing technology (F&AWMT). The framework, research fields and applications of IWMT are presented in figure 3. (Chen, 2015, p. 5–7.)

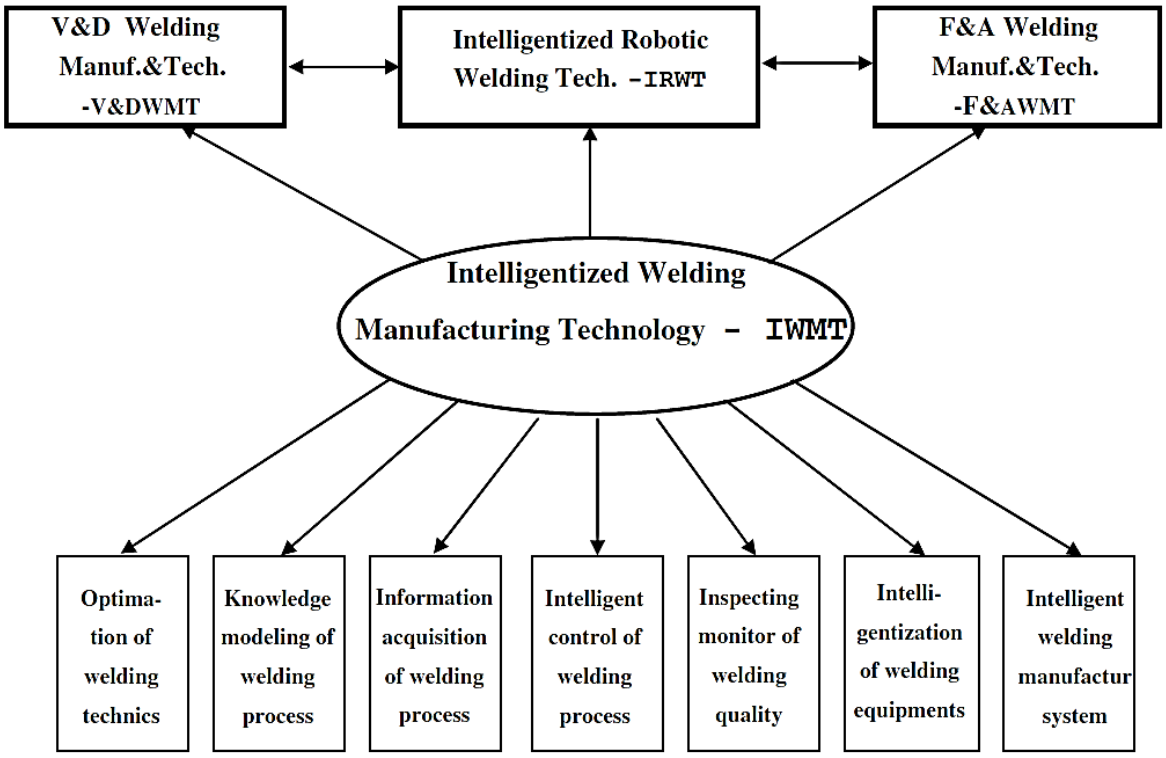

Figure 3. The framework of intelligent robotic welding technology (Chen, 2015, p. 6).

Adaptive welding also has adapted applications from modern artificial intelligence (AI) technology. The most important applications of artificial intelligence are related to neural networks and fuzzy logic, which are suitable for modelling complex nonlinear processes, such as arc welding and laser welding. As well, an adaptive welding station itself consists of several technological levels. The technological composition and the hierarchy of intelligent welding technology are illustrated in figure 4. (Chen et al., 2014, p. 118.)

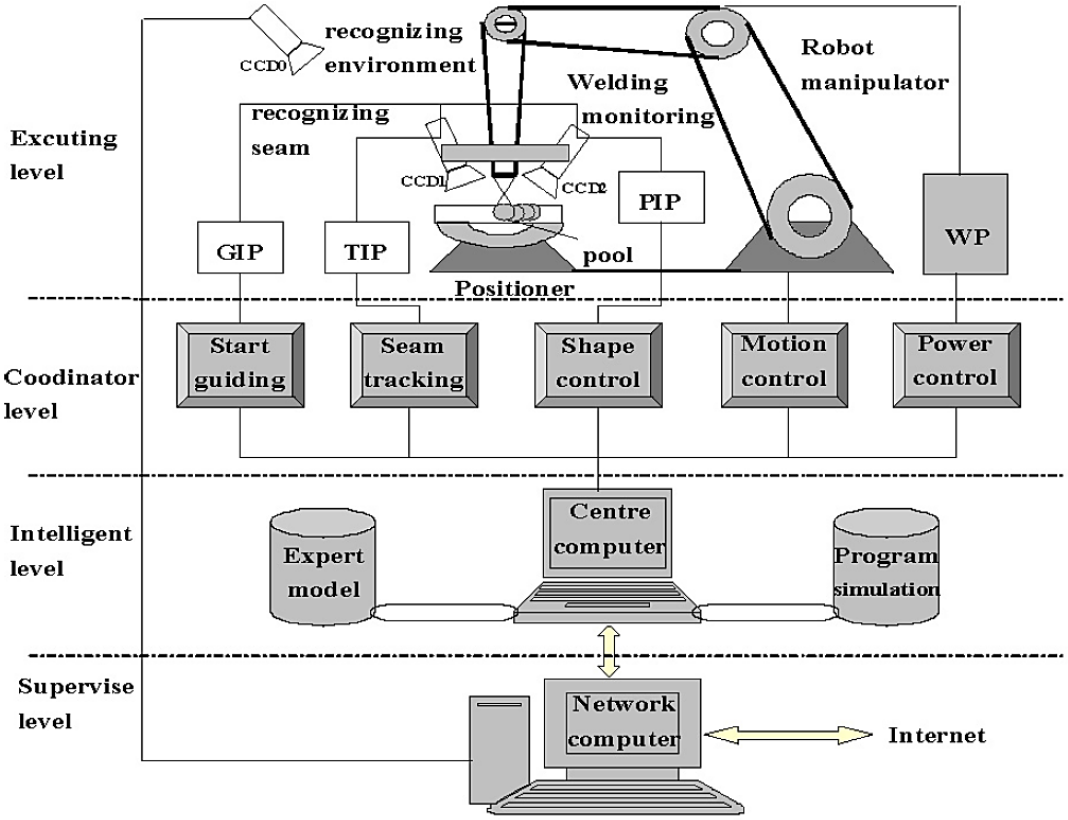

Figure 4. The technological levels of intelligent welding technology [in the figure, WP: welding power source, GIP: guiding image processor, TIP: tracking image processor, PIP: picture image processor, and CCD: charge coupled device] (Chen et al., 2014, p. 118).

Basically, the executing level of adaptive welding includes all essential welding equipment, including sensors and their image processors. The coordinator level includes all controllers coordinating welding process. The intelligent level includes the expert models of the welding process, virtual program simulator, AI and the centre computer. The supervise level is connected to the centre computer via internet access. (Chen et al., 2014, p. 118.)

2.4 Characteristics of development of adaptive welding

Generally, the development of an adaptive welding system has to begin with identifying the process related parameters and building a sensor system for monitoring these parameters. The final step is related to creating and testing an artificial intelligence, which controls the process in the future. Following steps are necessary to be considered while developing an adaptive welding system (Chen et al., 2014, p. 109–110):

1. Sensing and acquiring information of the welding process
2. Identifying the characteristics of the welding process
3. Developing an AI process controller.

The second step of identifying the characteristics in a robotic gas metal arc welding (GMAW) means also considering and classifying the GMAW process related parameters into three categories (Pires et al., 2006, p. 106–107):

1. Primary input variables that can be adjusted online during the welding
2. Secondary input variables that are defined before the actual welding job
3. Fixed input parameters that cannot be changed by the users.

The important basic parameters of GMAW process that affect the obtained welding result are: welding current (wire feed rate), polarity, arc voltage (arc length), travel speed, electrode extension (contact tip to work distance), electrode orientation (torch angle) and electrode diameter. (Olson et al., 1993, p. 575–576.) The primary variables of the GMAW process that can be adjusted online during the welding are the arc voltage, electrode feed rate together with the resulting current, and the travel speed. The secondary variables are set when the used welding process is selected comprising of the type of shield gas and the amount of gas flow, the torch angle and the type of the welding electrode wire. The fixed inputs include variables that cannot be altered such as the joint geometry, plate thickness and physical properties of the plate metal. For obtaining the desired quality as shown in figure 5, the primary parameters should be managed and monitored with some kind of feedback process controller. (Pires et al., 2006, p. 106–107.)

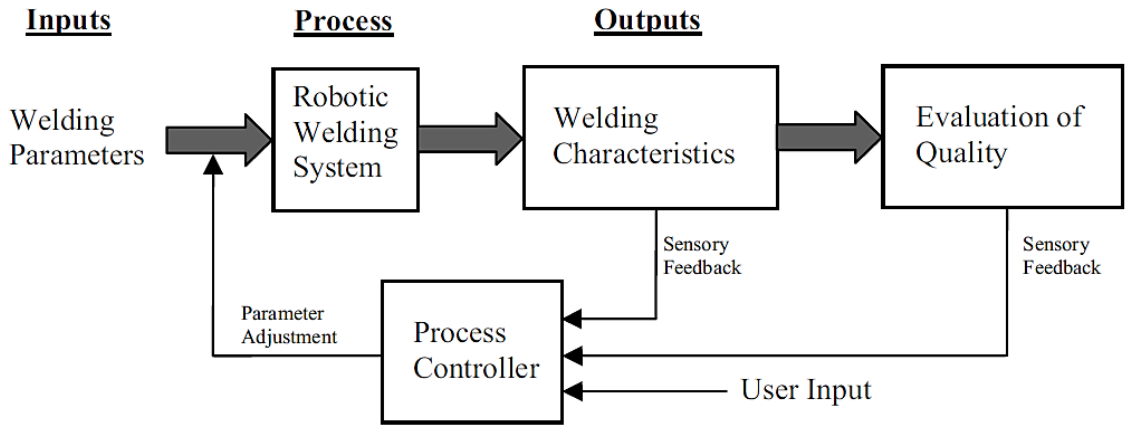

Figure 5. Overview of a robotic welding control system (Pires et al., 2006, p. 107).

All these input parameters should be considered and managed carefully to obtain acceptable results. The correct preparation of the setup and the selection of the secondary inputs are fundamental to efficient control of the primary inputs. (Pires et al., 2006, p. 107.) It must be realised that the parameters are not independent, for instance, wire feed rate affects welding current and hence the arc energy. Moreover, varying one parameter usually requires adjusting also another. (Olson et al., 1993, p. 575.)

2.5 The effect of GMAW parameters on weld attributes

The effects of GMAW parameters altering weld attributes, such as penetration, deposition rate, bead size and bead width in the usual welding situations is shown in table 1. However, the table shows only a general review for traditional welding situations. In special cases, the effect of one parameter may be stronger or weaker. (Olson et al., 1993, p. 575; Cornu, 1988, p. 232–237, 242–247, 262–264.)

Table 1. Effect of changes in GMAW variables on weld attributes (Olson et al., 1993, p. 575).

WELDING VARIABLES TO CHANGE	DESIRED CHANGES							
	PENETRATION		DEPOSITION RATE		BEAD SIZE		BEAD WIDTH	
	INCREASE	DECREASE	INCREASE	DECREASE	INCREASE	DECREASE	INCREASE	DECREASE
CURRENT AND WIRE FEED SPEED	INCREASE	DECREASE	INCREASE	DECREASE	INCREASE	DECREASE	LITTLE EFFECT	LITTLE EFFECT
VOLTAGE	NO EFFECT	NO EFFECT	LITTLE EFFECT	LITTLE EFFECT	LITTLE EFFECT	LITTLE EFFECT	INCREASE	DECREASE
TRAVEL SPEED	NO EFFECT	NO EFFECT	LITTLE EFFECT	LITTLE EFFECT	DECREASE	INCREASE	DECREASE	INCREASE
ELECTRODE EXTENSION	DECREASE	INCREASE	INCREASE(A)	DECREASE(A)	INCREASE	DECREASE	DECREASE	INCREASE
WIRE DIAMETER	DECREASE	INCREASE	DECREASE	INCREASE	LITTLE EFFECT	LITTLE EFFECT	LITTLE EFFECT	LITTLE EFFECT
SHIELD GAS %	INCREASE	DECREASE	LITTLE EFFECT	LITTLE EFFECT	LITTLE EFFECT	LITTLE EFFECT	INCREASE	DECREASE
GUN ANGLE	DRAG	PUSH	LITTLE EFFECT	LITTLE EFFECT	LITTLE EFFECT	LITTLE EFFECT	PUSH	DRAG

(A) WILL RESULT IN DESIRED CHANGE IF CURRENT LEVELS ARE MAINTAINED BY ADJUSTMENT OF WIRE FEED SPEED

The table 1, which was published in ASM Handbook of Welding, Brazing and Soldering states that arc voltage and travel speed have “No effect” on penetration, which is true in the usual cases (Olson et al., 1993, p. 575). However, in this study, arc voltage and travel speed were found effective for fine adjusting penetration while welding relatively thin 5 mm steel sheets together without backing. Generally, thin sheets are more sensitive to heat input, thereby arc voltage might be considered to have an effect on penetration. As well, travel speed can be used for fine adjusting the penetration, even if only within certain limits. It should be kept in mind that for every welding case there is only one optimum operating zone or quality window which produces stable weld pool without spatters. (Cornu, 1988, p. 232–237, 242–247, 262–264.)

2.5.1 Welding current and wire feed rate

The current has the most significant influence on the deposition rate and therefore on the shape of the weld. GMAW is based on a constant voltage power source, hence when wire (electrode) feed rate is altered the welding current varies while the arc voltage remains almost the same. Since welding current and wire feed rate are interdependent, an increase in current means more wire fused per unit of time resulting greater penetration and weld pool size, while bead width remains almost the same. In addition, the polarity of the welding torch has an effect on weld attributes. Usually mainly direct current, electrode positive (DCEP) is used, because it provides a stable arc, low spatters, a good bead profile and greater

penetration when compared to alternative direct current, electrode negative (DCEN) setup. (Olson et al., 1993, p. 575–576; Cornu, 1988, p. 228–229.)

2.5.2 Arc voltage

Arc voltage is traditionally considered primarily affecting to bead width, and not having significant effect on other weld attributes such as penetration. Increasing the arc length makes the arc higher and wider and hence it widens the bead. Generally, when welding with high amperes, arc voltage has less than 1 mm effect on penetration. Since the arc voltage can be varied only a few Volts, it does not such a significant effect on penetration as current. And even though an increase in voltage increases the heat input as well, it may usually simply dissipate. However, when welding thin sheets with low current, the effect of arc voltage is more significant. Thereby, altering the arc voltage for fine adjusting the penetration and the bead shape might be important in certain welding cases. However, it must be realised that excessively high arc voltage can cause imperfections, such as porosity, spatters and undercut. (Olson et al., 1993, p. 575; Cornu, 1988, p. 235–237.)

2.5.3 Travel speed

Travel speed has a great impact on bead size together with wire feed rate. These two parameters should be considered in relation and adapted to particular welding conditions. If travel speed is reduced the bead becomes wider, flatter and smoother, because more filler material is deposited per unit of length. Correspondingly, if travel speed is increased the bead becomes narrower, higher and sharper. The effective depth of penetration increases slightly at first and at very low speeds suddenly reduces as the molten pool is flooding forward and weakening the penetrative effect of the arc. The travel speed and wire feed rate that cause maximum penetration can only be verified by tests. (Olson et al., 1993, p. 576; Cornu, 1988, p. 242–245.)

2.5.4 Electrode orientation

Electrode orientation is defined as an angle between the welding torch and the normal of the welding surface, as well the direction of travel. Trailing travel angle (“pulling welding”) of 5 to 15° provides maximum penetration and a narrow, convex bead surface. Leading travel angle (“pushing welding”) provides flatter bead profile and good weld pool protection. The trailing travel angle is better adapted to axial spray transfer (long arc) and the leading travel

angle is better adapted to short-circuit transfer, and therefore to the welding of thin sheets. (Olson et al., 1993, p. 576; Cornu, 1988, p. 249–250.)

2.5.5 Electrode extension

Electrode extension is the distance between the last point of electrical contact (usually the contact tip of the welding torch) and the end of an electrode wire. The true electrode extension is hard measure as true arc length between the end of the electrode and the work object surface is difficult to measure be accurately. Alternatively, easily measurable contact tip to work distance (CTWD) can be used for estimating the effect of the length of electrode wire. An increase in the electrode extension causes a greater amount of metal deposited by the energy of the Joule effect, resulting in a higher and narrower weld bead. Shorter electrode extension results in a higher current and a greater penetration. In addition, the electrode extension affects metal transfer mode (short-circuit, axial spray and globular transfer) due to the influence of the Joule effect. The recommended CTWD in GMAW is usually between 10 and 35 mm depending on the electrode type, the application and the desired metal transfer mechanism. (Olson et al., 1993, p. 576; Cornu, 1988, p. 257–258.)

2.5.6 Electrode diameter

The electrode wire diameter affects the weld bead composition. A thicker electrode wire requires higher minimum current for achieving the same metal transfer characteristics than a thinner electrode. However, a higher current causes greater deposition and deeper penetration. Nevertheless, position welding applications may prevent the use of some electrodes. (Olson et al., 1993, p. 576.)

2.5.7 Shield gas type and flow rate

The composition and flow rate of shield gas are fixed parameters, affecting welding attributes, such as metal transfer mode, depth of fusion, weld bead attributes, travel speed and cleaning action. Metal inert gas welding (MIG) process consumes inert shield gas, usually argon (Ar). Metal active gas welding (MAG) process consumes active shield gas, usually a mixture of carbon dioxide and argon (CO_2 + Ar). (Olson et al., 1993, p. 580.) The flow of shield gas must be determined carefully, as inadequate flow results in turbulence and the introduction of air, predisposing the weld to porosity. Correspondingly, a too great a flow

may also generate turbulence, drawing in air and predisposing the weld to porosity again. (Cornu, 1988, p. 258–258.)

2.6 Arc energy

The arc energy defines an amount of energy transferred to the workpiece by welding. Arc Energy (E), calculated as in upcoming equation, is dependent on welding current, arc voltage, and travel speed (Olson et al., 1993, p. 1075; Cornu, 1988, p. 178):

$$E\ \left(\frac{kJ}{mm}\right) = \frac{Welding\ current\ (A) \times Arc\ voltage\ (V)}{Travel\ speed\ \left(\frac{mm}{s}\right) \times 1000} \quad (1)$$

Arc energy has to be considered at least when welding materials with metallurgical properties delicate to the amount of energy input, such as high strength steels. Arc energy can be converted to heat input by multiplying by the specific heat-transfer efficiency factor. However, arc energy also has a significant effect on the resulted weld attributes together with the energy of metal drops transferred from the electrode. Thereby, arc energy might be considered a factor among other variables while developing an adaptive welding system. (Olson et al., 1993, p. 119–123, 1075, 2695, 2803.)

3 ARC WELDING SENSORS

This chapter describes modern sensors used for sensing arc welding processes. The arc welding sensors can be classified to contact and non-contact sensors, as well geometrical and technological sensors. Geometrical sensors can include seam tracking sensors. Technological sensors are related to the primary process variables, for instance, current, voltage and wire feed sensors. Due to high temperatures and the demand for accuracy and response, state-of-art welding process sensors are often non-contact and digital. (Garašić, Kožuh & Remenar, 2015, p. 1069–1070, 1973.)

3.1 Arc voltage sensors

To obtain the best results in sensing the arc voltage, the measurement should be made near the welding arc. The contact tube conveys the welding current to the electrode wire and someone could propose the contact tube as a good place for arc voltage measurement. However, the actual arc voltage is approximately 0.3 V higher than the measured voltage at the contact tube. In practise, measuring true arc voltage is difficult if not impossible. A more reliable method is locating the voltage sensor directly on the electrode wire inside the wire feeding unit. (Pires et al., 2006, p. 75–76; Garašić et al., 2015, p. 1070.)

3.2 Welding current sensors

Generally, two types of sensors are used for the measurement of the welding current: Current Shunt and Hall Effect (Pires et al., 2006, p. 76; Garašić et al., 2015, p. 1070).

3.2.1 Current Shunt

The core component of a current shunt is a resistor, through which the current is conveyed. The current is measured as a dip in the voltage past the resistor, similar to the measurement procedure with a multimeter. However, the major drawback of this simple method is sensitivity to noise due to small dynamic measurement range. (Pires et al., 2006, p. 76; Garašić et al., 2015, p. 1070.)

3.2.2 Hall Effect sensor

The Hall Effect has a current cable run though its circular cast iron core. The actual device is located at the top of the iron cast measuring changes in the magnetic field and its currents. The Hall Effect has the advantage being non-contact and disruption-free. (Pires et al., 2006, p. 76; Garašić et al., 2015, p. 1070.)

3.3 Wire feed rate

Wire feed rate is an important control parameter in obtaining a steady welding process, hence it also affects the welding current due to the constant voltage and the synergy technologies of modern GMAW power sources. In robotic applications, wire feed unit is usually installed at the top of the actuator giving reliable push due to close distance to the torch. However, measuring wire feed rate with an independent sensor ensures proper functionality of the feeding equipment and thereby ensures resulted quality. (Pires et al., 2006, p. 76–77; Garašić et al., 2015, p. 1070.)

3.4 Optical sensors

Optical sensors are an alternative for contact seam tracking, for example through-arc sensing. The optical sensors are faster and provide more information than contact geometrical sensors. However, they are more expensive and complex than the simple contact sensors. (Garašić et al., 2015, p. 1071–1073.)

The optical geometrical sensors are generally laser scanners, non-contact sensors, based on laser triangulation. A laser beam sweeps the measured surface in linear or circular motions and an imager captures data from the reflection of the laser. The principle of laser triangulation is illustrated in figure 6. (Pashkevich, 2009, p. 1034; Pires et al., 2006, p. 78–79.)

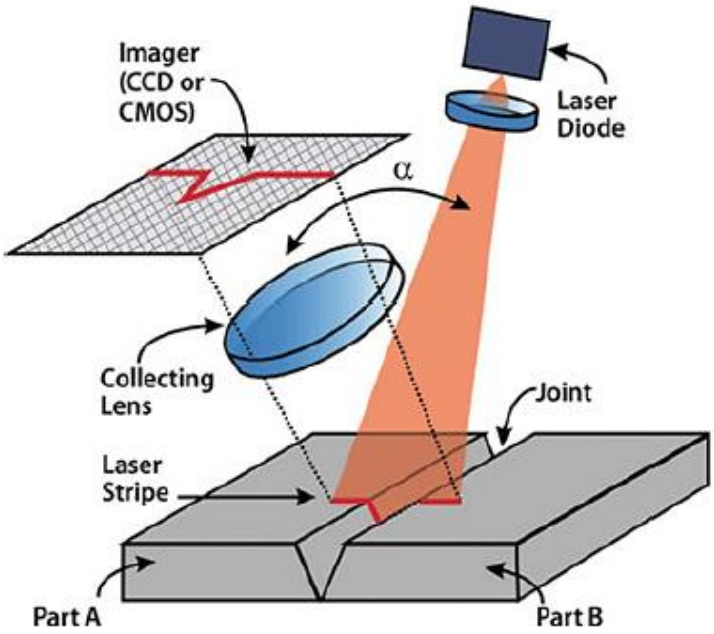

Figure 6. The principle of laser triangulation (Juneghani & Noruk, 2009).

Basically, laser scanning is measuring distances from multiple points and creating a model of the measured surface. The imagers are either charge-coupled devices (CCD) or complementary metal oxide semiconductors (CMOS). The sensor acquires two-dimensional (2D) information of the groove width and depth as a group of coordinates. During the welding, when the sensor is moving, a three-dimensional (3D) profile of the weld can be created. (Pires et al., 2006, p. 79–83; Garašić et al., 2015, p. 1071.)

A typical laser scanning sensor has a scan sweep frequency of 10–50 Hz and an accuracy of at least ±0.1 mm, which is more than sufficient for most welding processes. However, some high travel speed cases may require a faster scanning rate. Moreover, it should be kept in mind that single scans may generate outlier errors due to perturbations and reflections caused by the welding process and the highly reflective metallic surfaces. Laser scanners are reliable and accurate sensors that have good enough capabilities within welding process. However, they need to be attached to the welding torch, taking some place and limiting reachability. Laser scanners are also relatively expensive, costing approximately 40,000 € a piece. (Pires et al., 2006, p. 83–84; Garašić et al., 2015, p. 1071–1072.)

One product example of a laser sensor is Meta's Smart Laser Sensor SLS-050, introduced in 2009. The sensor can acquire geometrical data with a framerate of 30 fps (frames per second) and locate within the accuracy of ±0.1 mm. Network connection enable real-time process monitoring and controlling by guiding used welding robot or manipulator. The sensor is cooled by flowing compressed air. This type of a sensor can be used for seam finding and seam tracking as well as for measuring groove geometry. (Meta Vision Systems, 2012; Meta Vision Systems, 2014.)

3.5 Infrared sensors

Since welding is a thermal process, non-contact infrared imaging is ideal for sensing welding information, especially crucial parameters such as heat transfer, predicting joint depth penetration and bead width of a weld. Thermographic infrared sensing using infrared (IR) sensors is a predominant and widely used method for sensing, monitoring and controlling the welding process. The basic principle of infrared thermography (IRT) is that a proper weld would generate a temperature distribution on the surface that shows a regular and repeatable pattern. Perturbations in weld attributes, such as penetration and variations in welding conditions should be seen as notable changes in the thermal profiles. (Chokkalingham, Chandrasekhar & Vasudevan, 2012, p. 1996; Alfaro, 2011, p. 88.)

In the past, various configurations of thermocouples were used for monitoring temperature distributions during welding processes. However, the slow response and low spatial response of thermocouples are problematic in their use for process control. Thermal changes during welding are quick, so a more responsive thermal monitoring method was needed and infrared sensing ousted thermocouples. Infrared (IR) sensing is superior when compared to standard techniques, such as thermocouples. The advantages of IR cameras are contactless temperature field measurement, true multidimensional view, high sensitivity (down to 20 mK) and low response time (down to 20 µs). (Chokkalingham et al., 2012, p. 1996; Carlomagno & Cardone, 2010, p 1187.)

Infrared sensing is based on measuring electromagnetic radiation in IR spectral band, emitted from the body surface. In welding processes, IR sensing is used for measuring surface temperatures from the weld pool and plasma or alternatively from the solidified, but still glowing weld. It has to be remembered, that infrared sensing measures only surface

temperatures, not internal temperatures. IR sensing can be carried out by using dot, line and image analysis techniques. The dot analysis is the lightest technique to compute, but it cannot provide a multidimensional view. The line and image analysis techniques enable acquisition of a multidimensional thermal distribution on a weld surface for more comprehensive analysis. (Alfaro, 2011, p. 88; Chokkalingham et al., 2012, p. 1996.)

3.5.1 Basic radiative heat transfer theory

Heat transfer by radiation is an energy transfer mode that occurs as electromagnetic waves. The movement of charged protons and electrodes result in electromagnetic radiation, carrying energy away from the body surface. All bodies, even liquid, and gas emit this electromagnetic radiation at temperatures above absolute zero. Depending on the characteristics of the material, electromagnetic energy can be also reflected and/or absorbed by a body as well as passed through. The amount of thermal radiation being emitted or absorbed depends on the material characteristics, surface finish, thermodynamic state of the material (temperature) and the specific wavelength of the electromagnetic wave considered. (Carlomagno et al., 2010, p. 1188–1190; Astarita & Carlomagno, 2013, p. 5–6.)

Important approaches to the theory of electromagnetic radiation are the Planck's law and the blackbody concept. The blackbody is an idealized solid body that absorbs and emits all incident electromagnetic radiation. (Astarita et al., 2013, p. 5–6.) Planck's law, originally proposed in 1900, defines the amount of electromagnetic energy emitted from a black body as a function of wavelength. It is known as the spectral hemispherical emissive power $I^b(\lambda)$ [W/m^2]. The Planck's law is presented in upcoming equation:

$$I^b(\lambda) = \frac{C_1}{\lambda^5(e^{C_2/\lambda T} - 1)} \quad (2)$$

in which λ is the radiation wavelength (m), T the absolute black body temperature (K), *e* is the Euler's number and C_1 and C_2 are the first and the second universal radiation constants (equal to 3.7418×10^{-16} Wm^2 and 1.4388×10^{-2} mK). The Planck's equation shows that the spectral hemispherical power (I^b) goes to zero when the wavelength is approaching to zero or infinity ($\lambda\rightarrow0$ or $\lambda\rightarrow\infty$). We have to pay attention to the fact that for a black body, the

intensity of radiation is independent on the angle of radiation. (Planck, 1900, p. 202–204; Carlomagno et al., 2010, p. 1188–1190.)

The electromagnetic spectrum (shown in figure 7) is divided into different wavelength intervals, called spectral bands or just bands. The thermal radiation includes the spectral bands of infrared, visible light and ultraviolet. (Astarita et al., 2013, p. 6.)

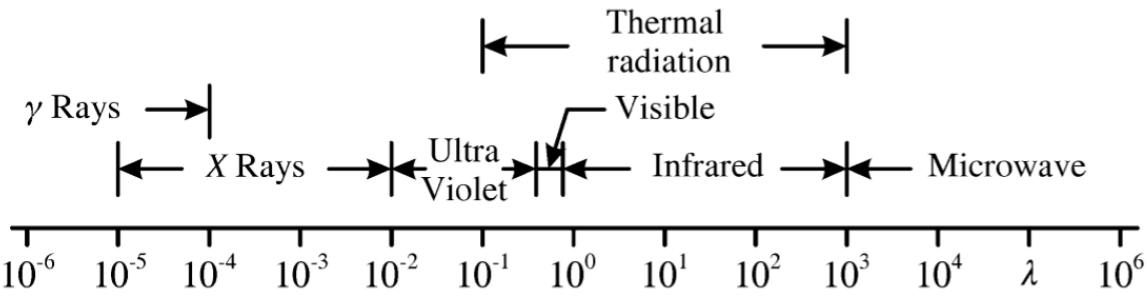

Figure 7. Electromagnetic spectrum [wavelength λ in μm] (Astarita et al., 2013, p. 6).

The infrared band can be further sub-divided into four bands, called: near infrared (0.75–3 μm), middle infrared (3–6 μm), far or long infrared (6–15 μm) and extreme infrared (15–1000 μm). Most IR camera (2D) detectors are sensitive in the middle (MWIR) or the long wavelength (LWIR) band, although some more specialised detectors use the near infrared (NIR) band. (Carlomagno et al., 2010, p. 1189.)

The real objects emit significantly less electromagnetic radiation than the theoretical black body at a similar wavelength and temperature. However, the Planck's law can be applied to a real body by introducing the spectral emissivity coefficient ε, which depends on the hemispherical emissivity power of the black body and the corresponding hemispherical emissivity power I(λ) of the particular real body, such as defined in the following equation. (Carlomagno et al., 2010, p. 1189.)

$$\varepsilon(\lambda) = \frac{I\,(\lambda)}{I^{b}(\lambda)} \tag{3}$$

Thereby, the Planck's equation (2) can be adjusted for real bodies, as presented in upcoming equation, by multiplying its second term by ε(λ):

$$I(\lambda) = \varepsilon(\lambda) \frac{C_1}{\lambda^5 (e^{C_2/\lambda T} - 1)} \quad (4)$$

However, the emissivity of real bodies, such as especially metals, is usually dependent on the viewing angle and wavelength. These factors should be considered to obtain the best possible results on IR applications. (Carlomagno et al., 2010, p. 1189–1190.)

3.5.2 Accuracy of IRT when measuring metals

Measuring metallic objects is challenging because their emissivity is usually low compared to 0.8–0.9 of the grey body materials, such as wood and plastics. Metallic bodies not only emit less but also reflect a large amount of ambient radiation. Therefore, metals are not the best measurable materials for standard IR cameras. However, despite all these problems, metallic materials can be accurately measured at high temperatures (600–1500 °C), when a short waveband (NIR) detector is applied. This is based on the physical fact that at high temperatures the energy of emitted thermal radiation is greatest at the shorter wavelengths as shown in figure 8. (Carlomagno et al., 2010, p. 1189; Astarita et al., 2013, p. 9–10, Schiewe & Schindler, 2013, p. 1–2; Gruner, 2003, p. 12.)

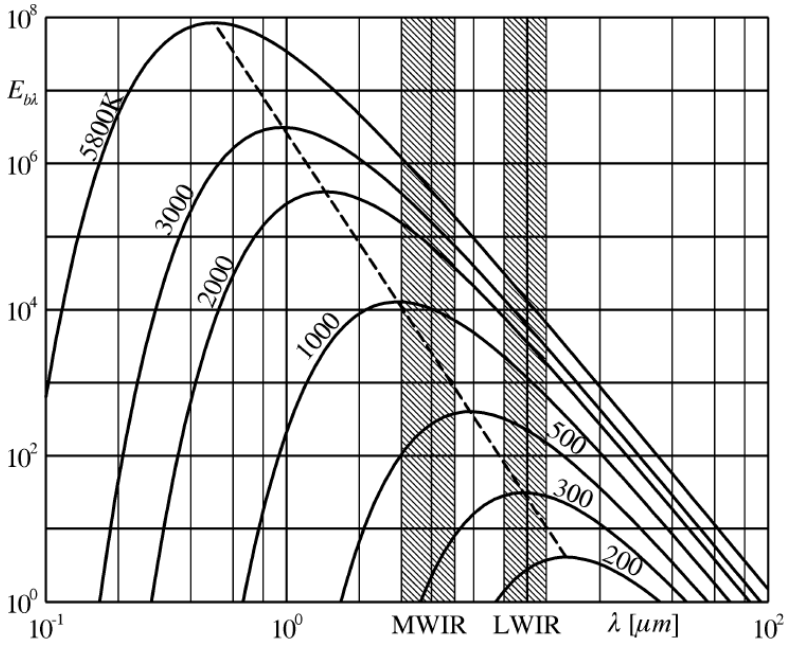

Figure 8. Spectral hemispherical emissive power of a black body [W/m^2 µm] in vacuum for various absolute temperature values [K] as a function of the wavelength [λ] (Astarita et al., 2013, p. 9).

Additionally, short waveband NIR detectors have the benefit being tolerant to the error of varying emissivity as shown in table 2 (Schiewe et al., 2013, p. 1–2; Gruner, 2003, 12).

Table 2. Temperature measurement error [ΔT_O] and relative temperature measurement error [$\Delta T_O/T_O$] at an emissivity setting error of 10 % dependent on object temperature and spectral band (Shiewe et al., 2013, p. 2).

Spectral range	$T_O = 600$ °C		$T_O = 800$ °C		$T_O = 1200$ °C	
	ΔT_O	$\Delta T_O/T_O$	ΔT_O	$\Delta T_O/T_O$	ΔT_O	$\Delta T_O/T_O$
0,8 µm to 1,1 µm	5 °C	0,9 %	8 °C	1,0 %	15 °C	1,3 %
1,5 µm to 1,8 µm	9 °C	1,5 %	13 °C	1,7 %	25 °C	2,1 %
3 µm to 5 µm	20 °C	3,4 %	30 °C	3,8 %	57 °C	4,8 %
8 µm to 14 µm	48 °C	7,9 %	72 °C	9,0 %	136 °C	11,3 %

Basically, NIR sensors would have only about 1 % measurement error, even if there is a 10 % error at emissivity setting value. This explains why IR sensors dedicated for measuring metals at high temperatures are short waveband NIR detectors rather than MWIR or LWIR detectors. By understanding the radiation theory, IR sensor can also be accurate for measuring metals if essential variables, such as emissivity of the object material, waveband and angle are considered. (Schiewe et al., 2013, p. 1–2; Gruner, 2003, 12; Carlomagno et al., 2010, p. 1189–1190.)

3.5.3 Technologies of IR radiation detectors

The core component of an IR camera is the radiation detector. Radiation detectors can be classified into two technological groups: thermal detectors and quantum detectors. The thermal detectors are made of a metal compound or a semiconductor that is sensitive to the energy flux of infrared radiation. The sensitivity of quantum detectors is based on photon absorption. The quantum detectors are usually more sensitive than thermal detectors. However, quantum detectors require a strong cooling and are more expensive than thermal detectors. Typical IR detectors can measure up to 1500 °C, and the measurement range can be improved further by filtering the ongoing radiation. (Carlomagno et al., 2010, p. 1190–1191; Astarita et al., 2013, p. 29–35.)

3.5.4 Filtering of thermographic images

Infrared sensing the molten weld pool requires filtering the unwanted thermal emissions, such as the interference of arc radiation and welding electrode emission. The filtering is done by ignoring the wavelength range of the arc, for example by scanning the infrared sensor with a spectral response greater than 2 µm or by using CCD cameras with specific band pass filters. (Chokkalingham et al., 2012, p. 1996.) Spatters may also require filtering because they cause unwanted "Salt and Pepper noise" type temperature spikes to thermal profile distributions (figure 9).

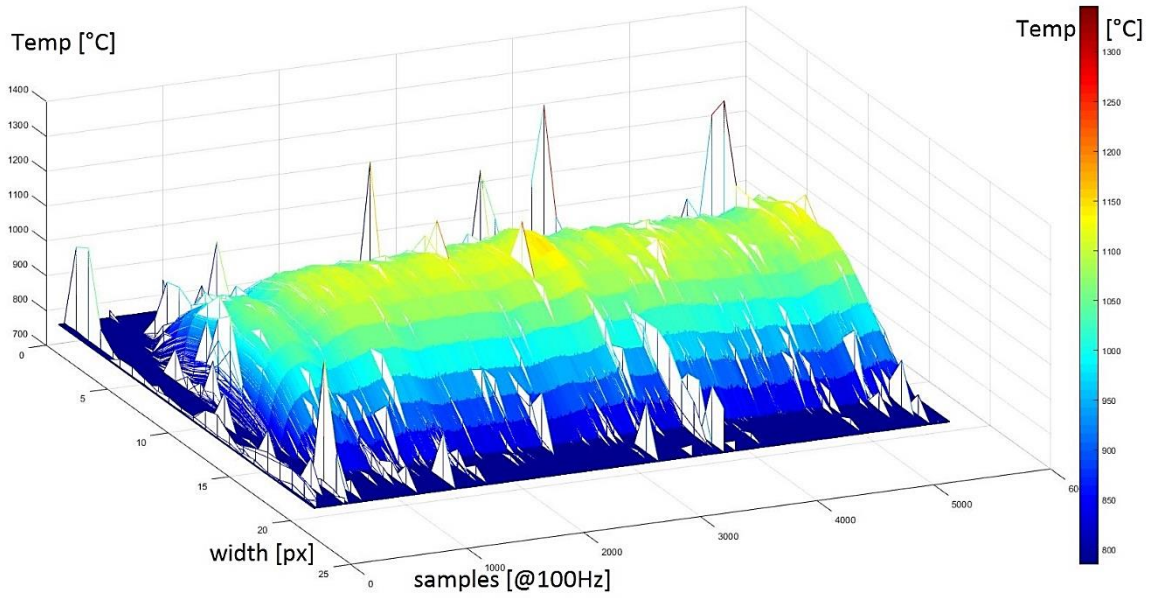

Figure 9. Spatters and perturbations in unfiltered thermal profile distribution.

Spatters can be filtered out from measurements by using median filters (for example "medfilt2" function in MATLAB). Median filtering is based on going through the signal, entry by entry, and replacing the value of each entry with the median of the neighbouring entries. The same thermal profile distribution, as in figure 9, is shown with median filtering and slight scaling in figure 10.

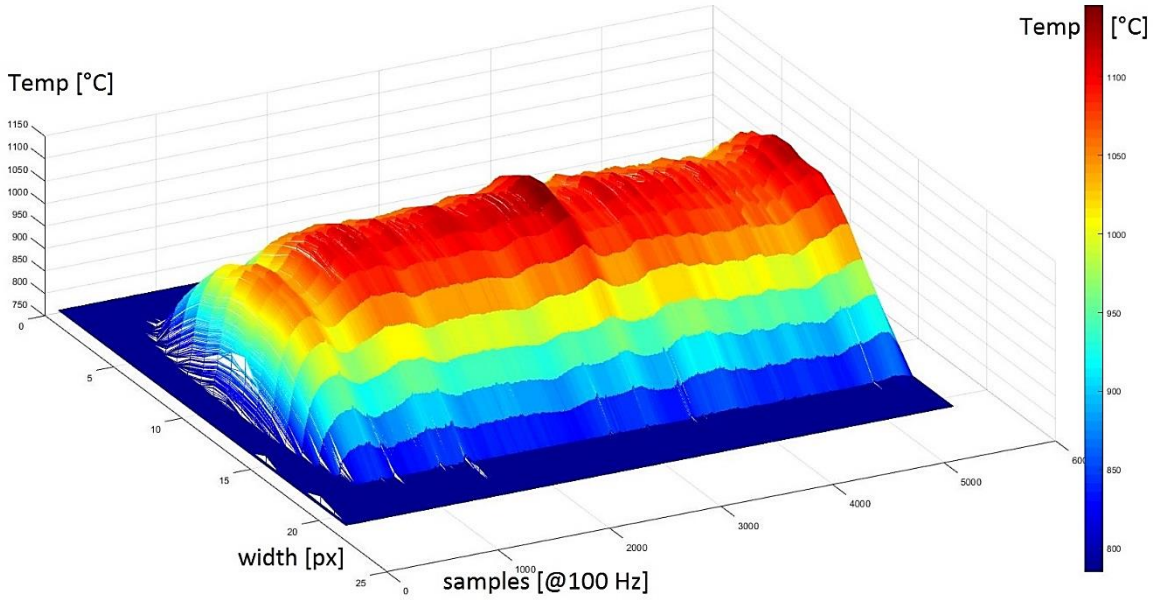

Figure 10. Median filtered thermal profile distribution.

As seen in figure 10, the median filtering results in a smooth and perturbation free thermal profile. The neighbourhood entry size was able to be kept small enough, thereby the filtering result was good and essential details were retained.

3.5.5 ThermoProfilScanner

HKS-Prozesstechnik has recently developed an infrared thermal field monitoring device ThermoProfilScanner (TPS) for almost real time weld quality monitoring. The device tracks the area of the thermal field after the welding torch at a framerate up to 400 fps, allowing recordable travel speeds up to 180 m/min. Hence, thermal field has a direct relation to seam attributes, and imperfections such as lack of penetration, offset and holes can be identified. (HKS-Prozesstechnik, 2016a.) The principle of weld quality monitoring with TPS is illustrated in figure 11.

Figure 11. ThermoProfilScanner, a faulty brazed joint and the fault shown as an abnormal thermal profile (HKS-Prozesstechnik, 2016b).

ThermoProfilScanner is based on an optic less line type quantum detector, cooled and protected by flow of shield gas (Ar or CO_2). The TPS is sensitive at a spectral band of 0.8–1.1 µm (NIR), thus it has a very high measurement accuracy of about 0.2 % at the temperature of 1000 ºC. The recordable temperature range of TPS is 600–1350 ºC, at standard settings. TPS device variants can be calibrated to the emissivity of steel and stainless steel as well other metals, such as aluminium. When coupled with WeldQAS-device, TPS provides five pre-calculated thermal field attributes for every measurement, which are: max temperature, the width of temperature zone, symmetry, profile position and form differences. As Schauder et al. presented at the IIW (International Institute of Welding) 2013 conference, IRT by TPS had provided better results for inspecting penetration of induction welded pipes than conventional non-destructive testing (NDT) methods with electromagnetic testing and ultrasonic testing, of which the ladder did not reveal any defects while the former did. (Köhler, 2016; Köhler, 2015; Schauder et al., 2013.)

3.6 Non-destructive testing sensors

In addition to the standard welding process sensors, non-destructive testing methods by sensors can be applied for inspection of the weld quality behind the weld pool. These sensor-based NDT methods include visual inspection techniques, real-time radiography, ultrasonic imaging techniques, and eddy current testing. (Ithurralde et al., 2000; Zahran et al., 2013, p. 26–34.)

4 WELDING PROCESS CONTROL STRATEGIES

The welding process can be controlled either manually or automatically. An automatic welding process control requires a closed loop or feed forward control system with feedback control. The automatic feedback control can be built either by classical methods or intelligent methods. The classical welding control methods, such as applying a proportional-integral (PI) or proportional-integral-derivative (PID) controller together with a reference model are usable. As a drawback, these classical methods require precise mathematical modelling of the welding process which is challenging, because arc welding is generally a very complex multivariable process. In contrast, the intelligent control methods, such as neural networks and fuzzy logic, do not require accurate modelling of the welding process which explains why intelligent control strategies have been used in various applications. (Naidu, Ozcelik & Moore, 2003, p. 147–149, 160, 171–174; Einerson et al., 1992, p. 853–857; Tay & Butler, 1997, p. 61–69.)

4.1 Classical control methods

Arc welding processes can be controlled by using classical control methods such as PID control. As an example, Smartt and Einerson applied a PI controller to obtain desired heat and metal transfer in GMAW process with spray transfer mode. The difference between the welding current based on the reference model and the actual measured current was used as a feedback signal to obtain the correct wire feed rate and travel speed as presented in figure 12. (Smartt & Einerson, 1993, p. 217–229.)

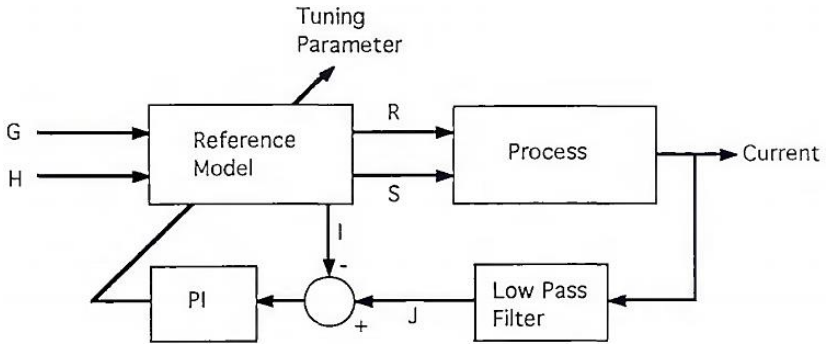

Figure 12. PI control of the GMAW process [in the figure, G: metal transfer, H: desired heat, R: travel speed, S: wire feed rate, I: model current and J: measured current] (Smartt et al., 1993, p. 220).

4.2 Intelligent control methods

Modern machine intelligence is based on soft computing methods such as neural networks, fuzzy set theory, genetic algorithms and simulated annealing, because they perform well on complex, non-linear cases when classical rule-based systems struggle. A neural network is a classifier and/or pattern recogniser which can be taught or adapted to complex processes when enough teaching data is provided. Fuzzy logic simulates human logic to make if-then rules, such as describing ages to young, teenager, middle-aged, quite old etc., which is difficult to be done with two-value or rule-based logic. Thereby, fuzzy sets have been applied to knowledge representation. Genetic algorithms and simulated annealing can be applied to systematic random search when the search space is too large for an exhaustive search and too complex to be reduced. Artificial intelligence (AI) methods and techniques can be divided into (currently) four generations (Jang, Sun & Mizutani, 1997, p. 1–9):

1st (old) generation - Rule-based systems
2nd generation - Neural networks, fuzzy sets, etc.
3rd generation - Big data & correlation analysis
4th (next) generation - Integrated pre-processed heuristics.

Current AI techniques usually apply both fuzzy logic and neural networks. These neuro-fuzzy AIs are typically taught with big data sets and verified with correlations. Neuro-fuzzy systems have successfully been applied to complex non-linear cases, such as classifying species, controlling consumer electronics, financial trading as well as industrial process control. However, it is usually difficult to explain how and why a neuro-fuzzy system makes its decisions. In addition, teaching and testing a neuro-fuzzy system is a slow process and a correlation does not automatically mean causation. That is why the next generation AIs are proposed to include pre-processed heuristics used to explain these issues. (Jang et al., 1997, p. 1–9; Tay et al., 1997, p. 61–69.)

4.2.1 Basic principle of neural networks

Neural networks are a class of modelling tools inspired by biological neural networks of the brain. A neural network is based on linked nodes that feed the input signals forward as illustrated in figure 13. The number and the structure of nodes and layers can be varied. Each node has built in node function, weight and threshold (bias) that define how the input signal is sent forward. (Jang et al., 1997, p. 199–205.)

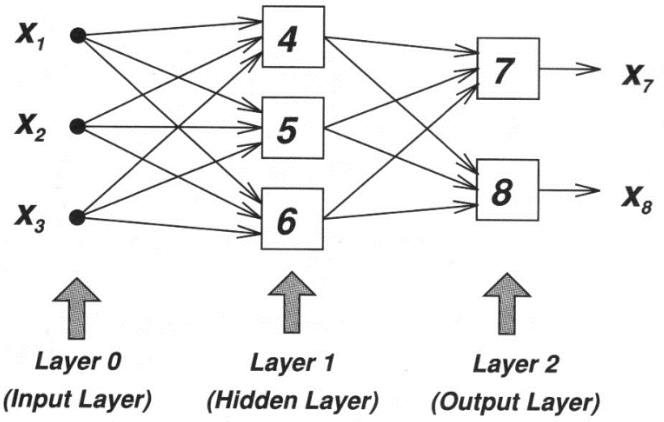

Figure 13. A 3-3-2 neural network (Jang et al., 1997, p. 205).

Usually, neural networks are taught by the procedure of backpropagation. The backpropagation is based on finding a gradient vector in the structure of a neural network. Once the gradient vector is found, various derivation based optimization and regression techniques can be applied for adjusting the node parameters. Basically, the input signal is fed back to the neural network several times. After each iteration, the actual output signal is compared to the desired output and the error signal is presented back to the neural network. The desired output is obtained by adjusting the weights of the nodes by the error signal and the teaching algorithm. (Jang et al., 1997, p. 205–210.) A number of pre-programmed neural network tools are available, as an example in MATLAB-software.

4.2.2 Performance of neural networks

The advantage of the neural network compared to linear and non-linear models in an example case of predicting the welding current can be seen in figures 14, 15 and 16, presented as regressions of predicted currents and measured currents. (Carrino et al., 2007).

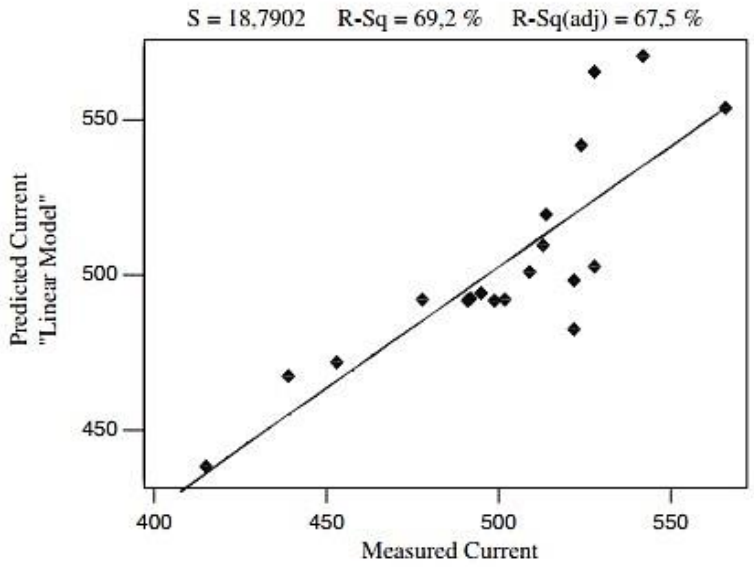

Figure 14. Measured current and predicted current using linear model (Carrino et al., 2007, p. 466).

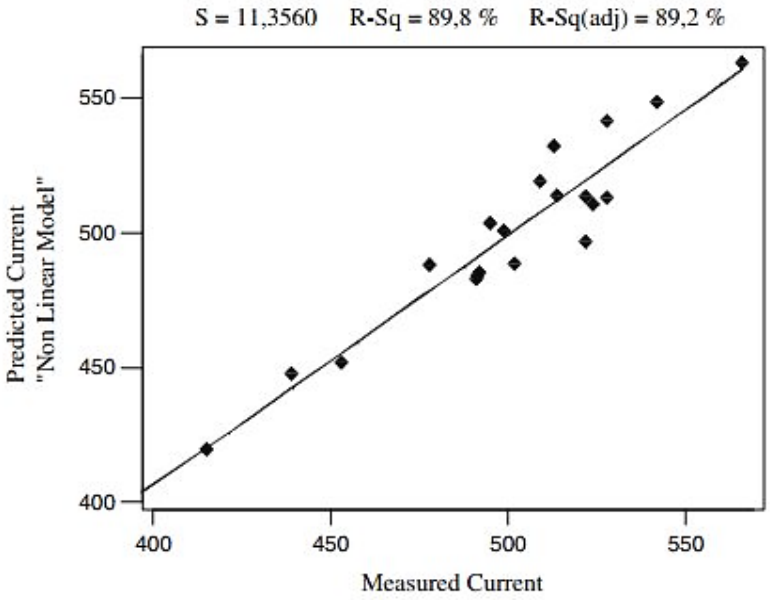

Figure 15. Measured current and predicted current using non-linear model (Carrino et al., 2007, p. 466).

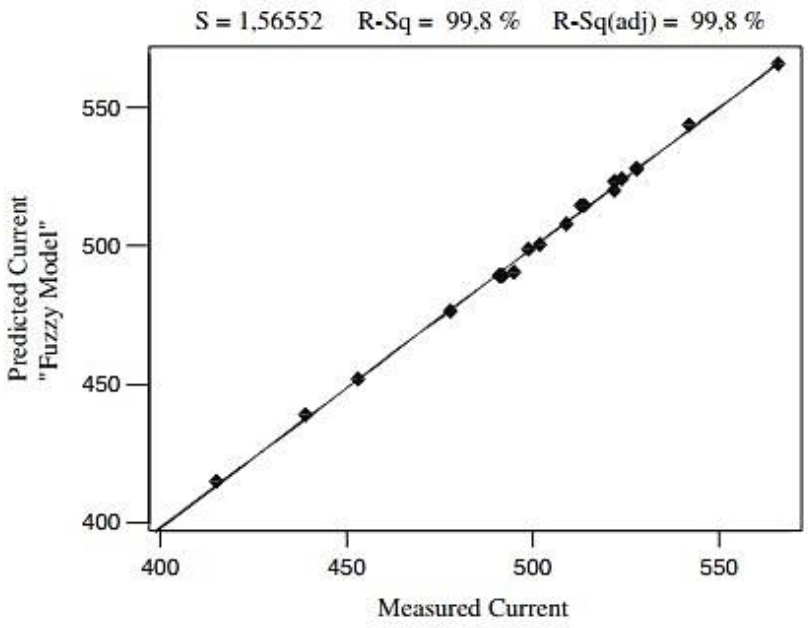

Figure 16. Measured current and predicted current using fuzzy model (Carrino et al., 2007, p. 466).

As it can be seen in figures, the neuro-fuzzy model performed well predicting the current very accurately. In this case, the regression of the neuro-fuzzy model is 99.8 % while the linear and the non-linear models have regressions equal to 69.2 % and 89.8 %. (Carrino et al., 2007, p. 466.)

5 STATE-OF-ART IN ADAPTIVE WELDING

Although adaptive welding has been studied for decades, there is still a lot of work to do. Generally speaking, sensing methods have evolved suitably fast and accurately for adaptive welding applications, but modelling the welding process itself still causes problems. (Heston, 2005, p. 42–44; Hägale, Nilsson & Pires, 2008, p. 963–971.)

5.1 Industrial examples

In the industry, adaptive welding is still not at the highest possible level. For example, while laser tracking is nowadays relatively standard method for automatic seam finding and seam tracking, it is questionable whether such applications can be called fully adaptive if the welding process itself is not automatically controlled. (Chen et al., 2014, p. 109–121; Mortimer, 2006, p. 272–276.)

5.1.1 Laser tracking in automotive industry

As an example, the car manufacturer Jaguar applied laser tracking to automatic MIG (metal inert gas) welding of aluminium C-pillars of XK sports car for the first time in 2006. The system was based on automatic seam finding and seam tracking. The system was also able to "adapt" to small variations of groove geometers by seam tracking. However, the welding parameters were possibly not adaptively controlled. (Mortimer, 2006, p. 272–276.)

5.1.2 Autonomous mobile welding robots

At least a few autonomous mobile welding robots, such as the so called NOMAD have been developed. Basically, these mobile manipulators aim to be more flexible than standard fixed welding robot cells and manipulators in specific cases when advanced reachability is needed. (Herman, Spong & Lylynoja, 2004; Chen et al., 2014, p. 120–121.)

5.1.3 Welding expert systems

As an example, a Finnish company specialised in welding automation has developed welding expert systems. This company's most advanced expert system "Weld Control 500 Adaptive" has some adaptive features such as automatic filling in multi-run welding. The system can be connected to welding equipment such as robot cells and seam tracking devices.

(Pemamek, 2015.) Expert systems and sensors are available for process monitoring as well, although feedback parameter correction is still a rare feature. These systems are usually more for quality monitoring than controlling the welding process itself. (Pemamek, 2015; HKS-Prozesstechnik, 2016c; Thermatool, 2016.)

5.2 Recent studies

The adaptability of welding has been studied with various welding processes and sensor types. Usually, several sensors have been applied simultaneously since welding is a multi-variable process. Predicting and controlling process parameters with neural networks has also been studied notably. (Chen, 2015, p. 3–34.)

5.2.1 Intelligent control of welding process parameters

Several configurations of neural networks and fuzzy logic have been found to bring good results in predicting process parameters, such as bead geometry and penetration depth. In these studies, a neuro-fuzzy control has been considered to be accurate enough for welding process control. However, a neuro-fuzzy approach still requires work in the teaching and testing stages. (Nagesh & Datta, 2002, p. 303–311; Xiong et al., 2013a, p. 743–745; Aviles-Viñas, Lopez-Juarez & Rios-Cabrera, 2015, p. 156–162.)

5.2.2 Current and voltage signals

Current and voltage are the basic parameters of the arc welding process which affect material deposition, heat input, penetration and bead size. Current is usually measured by a non-contact Hall-effect-sensor, based on induction. Voltage can be measured straight from wire feeding unit even if is it not the most accurate method for measuring the true arc voltage, also known as the arc length. (Pires et al., 2006. p. 75–76.)

An alternative and more accurate method for sensing arc voltage is based on acoustic emission analysis by a microphone and digital signal processing. Lv, Zhong, Chen and Lin (2014) found acoustic emission analysis to be an accurate method for measuring arc voltage within lengths of 3-7 mm in TIG (Tungsten inert gas welding) welding. Acoustic emission measuring has a potential for e.g. full penetration control when coupled with other sensing techniques. (Lv et al., 2014, p. 235–248.)

In addition, pulse welding signals have been studied with current and voltage sensors. (Pal, Bhattacharya & Pal, 2009, p. 1113–1129). Wang, Zhang and Wu (2012) developed a system for predicting penetration in pulse MAG welding, based on measuring features of the arc voltage signal. The study stated that measuring and adjusting the arc voltage during the pulse of a current can be used for controlling penetration in pulse welding. (Wang, Zhang & Wu, 2012, 233–237.)

5.2.3 Infrared sensing

In the early 1990's, Nagarajan, Chen and Chin (1989) proposed applying infrared thermography for sensing and controlling weld penetration, as they found a relation between the isotherms of the weld pool and the depth of penetration. Experiments were performed by IR camera, connected to a PC, and MAG welding process. As well, studies have been executed about IR filtering, since excluding perturbations caused by arc away from IR images is important. Usually, filtering is done by selecting a bandwidth that excludes the wavelengths of the arc. (Chen & Chin, 1990, p. 181–185; Nagarajan, Chen & Chin, 1989, p. 462–466; Chokkalingham et al., 2012, p. 1996.)

As a reference, Chandrasekhar, Vasudevan, Bhaduri and Jayakumar (2015) recently succeeded in estimating full penetration in TIG welding from thermographic images by employing neural network, fuzzy logic and an IR camera system. Root Mean Square (RMS) errors of predicted bead wide and penetration were considerably low, equal to 0.11 and 0.07. This result was achieved with 90 data, 70 of which were used for neural network training, 10 for checking and 10 for testing. The penetration estimation characteristics considered were: the weld pool IR width and IR length, the thermal area under Gaussian approximation of thermal profile as well as the welding current. (Chandrasekhar et al., 2015, p. 59–71.)

Other IR characteristics such as IR peak (maximum) temperature, mean & standard deviations of the Gaussian temperature profile, widths of thermography curves, and bead width estimations from the Gaussian temperature profiles have also been considered as potential characteristics to estimate weld penetration in other reference studies. However, applying these characteristics requires understanding the fundamentals of the weld pool thermal behaviour or alternatively again neuro-fuzzy methods. (Nagarajan et al., 1989, p.

462–466; Chen et al., 1990, p. 181–185; Chokkalingham et al., 2012, p. 1998; Ghanty et al., 2008, p. 396–397.)

5.2.4 Improved non-destructive testing methods

Applying NDT based techniques, such as ultrasonic, radiography and acoustic emissions has been studied as feedback signals in adaptive welding. As an example, non-contact laser ultrasonic probe has been developed allowing ultrasonic inspection during welding. An improved approach for weld defect identification from radiographic images has also been developed by neural network feature matching. (Hopko, Ume & Erdahl, 2002, p. 351–357; Zahran et al., 2013, p. 26–34.)

5.2.5 Vision sensing

Vision sensing is an extensively studied field of adaptive welding. Among laser seam tracking the variety of studies include specific cases such as visual inspection techniques, work object scanning, automatic seam recognition, weld pool size estimation and bead width measurement. The results of the studies show that modern camera technology together with a specific filter and image processing techniques is capable of monitoring hot and reflective metallic objects. (Chen, 2015, p. 21–22; Chen, Luo, & Lin, 2007, p. 257–265; Dinham & Fang, 2013, p. 288–300; Xiong et al., 2013b, p. 82–88.)

5.3 Future studies

The future research and development of adaptive arc welding are predicted to focus on the further improvement of artificial intelligence methods, expert systems, and intelligent modelling of the welding process. Still, a lot of research work is required to develop an efficient human brain like welding process controller and expert system. Similarly, various sensors need to be developed to be more accurate, robust and compact. (Chen et al., 2014, p. 109–111; Chen, 2015, p. 1–7, 21.) On the other hand, future studies of adaptive laser welding are expected to include the detection of internal imperfections, such as porosity, hot cracks and lack of fusion to be monitored with spectrometers and emission detectors. High sample rate sensors (over 10 kHz) and multi sensor integration are also expected to be studied. (You, Gao & Katayama, 2014, p. 194–198.)

6 EXPERIMENTAL SETUPS AND EXPERIMENTAL PROCEDURE

The usability and accuracy of an IRT sensor and a neural network in estimating full penetration was studied in the experimental part of the study. The motivation of the experiments was to find a clear relation between penetration and thermal profiles. Penetration estimating was the main reason why ThermoProfilScanner was acquired, although at first it needed to be adjusted to optimal measuring distance and the monitored parameters needed to be figured out. The experiments also complete a parameter library and expert system, essentially needed in adaptive welding. The neural network was selected as the control strategy of the welding process because further studies are likely to apply intelligent control strategies as well. Physical modelling of the welding process was considered to have benefits, though it was not applied in this study. The chronological workflow of the experimental procedure from preliminary testing towards adaptive application is explained step by step in figure 17.

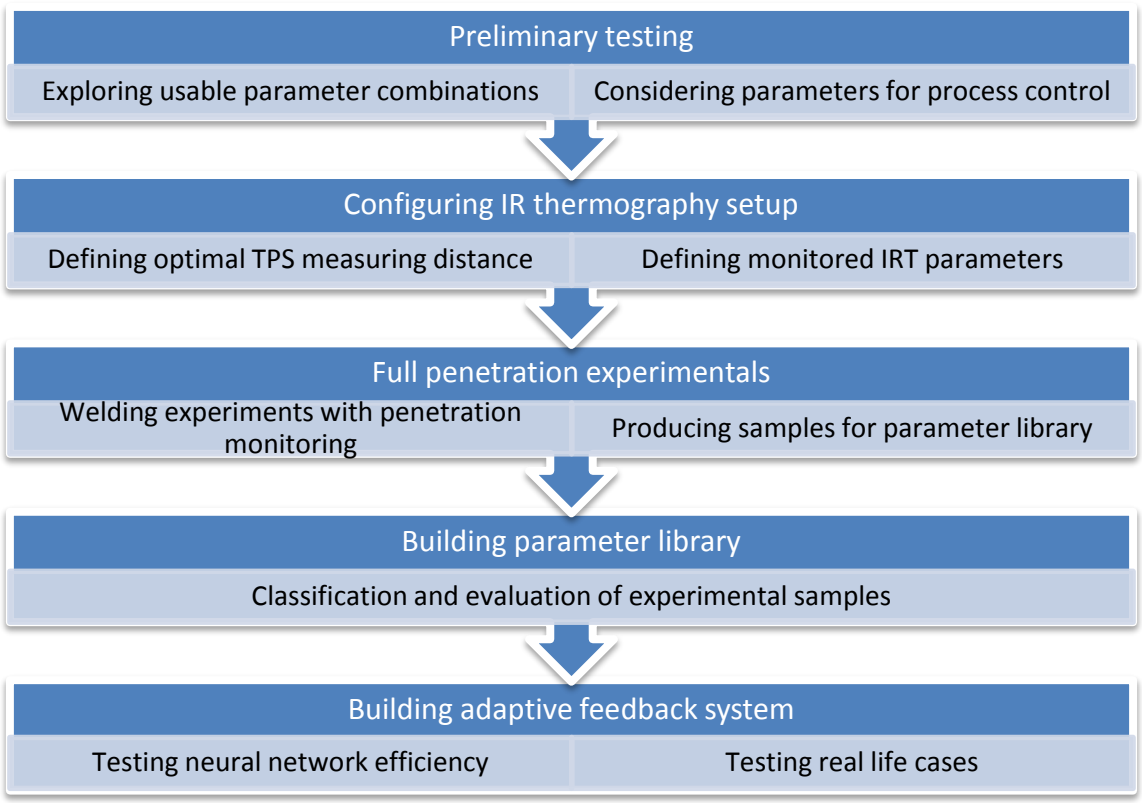

Figure 17. The workflow of the experimental procedure and the project.

At the preliminary testing stage, approximately 50 experiments were welded for exploring usable process parameter combinations. It was found that welding speed around 6-7 mm/s and wire feed rate of 9-10 m/min would be optimal for welding 5 mm thick steel plates with V-grooves and without backing. Arc length correction was also found useful for fine adjusting arc energy. However, at the preliminary testing stage, TPS was not optimally located causing further experiments described in this chapter necessary.

The measurement range of TPS, which is 600–1350 ºC, limits the installation position. The melting and the boiling points of steel are equal to about 1500 ºC and about 2850 ºC, hence the weld pool is expected to reach temperatures between these values. Thereby, if the measurement point of TPS is too close to the weld pool, the temperatures of the weld pool exceed the highest recordable temperature and the measurement is unusable. Correspondingly, if the measurement point is too far away from the weld pool the temperature is below the lowest recordable temperature. In addition, direct weld pool monitoring would require a strong filtering.

Later, TPS was configured so that it was able to record the maximum temperature of the thermal distribution. By making test welds and moving the TPS further away from the welding spot until temperatures did not peak over the measurement range, an optimal distance for the TPS could be defined. About 34 mm after the tip of the welding electrode was found as an optimal distance for the TPS measurement point. After this TPS configuration, the experimental setup was ready for full penetration experiments and following neural network teaching and testing stages. The ultimate goal of this project is to test real life welding cases with adaptive control as a follow-up for this study.

6.1 System layout

The adaptive welding station (figure 18) at Lappeenranta University of Technology (LUT) was built for fulfilling the preconditions needed in adaptive welding. The system layout consists of:

- Robot manipulator (ABB IRB-A1600)
- Robot controller (ABB IRC5 M2004)
- Power supply with network connections (Fronius Trans Puls Synergic 5000)
- Wire feeder (Fronius)

- Welding torch (Dinse DIX METZ 542)
- Collision sensor (Dinse DIX SAS 100)
- Positioner (NewFiro 800 HHT)
- Torch cleaning and calibration station (ABB TSC)
- Two laser sensors (Meta SLS 50 V1 with Meta Smart Laser Pilot system)
- HKS-Prozesstechnik ThermoProfilScanner and WeldQAS monitoring system
- Process sensor with current/voltage measurement (HKS-Prozesstechnik P1000)
- Gas sensor (HKS-Prozesstechnik GM30L 10B)
- Wire feed sensor (HKS-Prozesstechnik DV 25 ST)
- Master computer with ABB RobotStudio, Meta Laser Tools, SQL-server and custom made real time welding parameter adjustment program for adaptive welding.

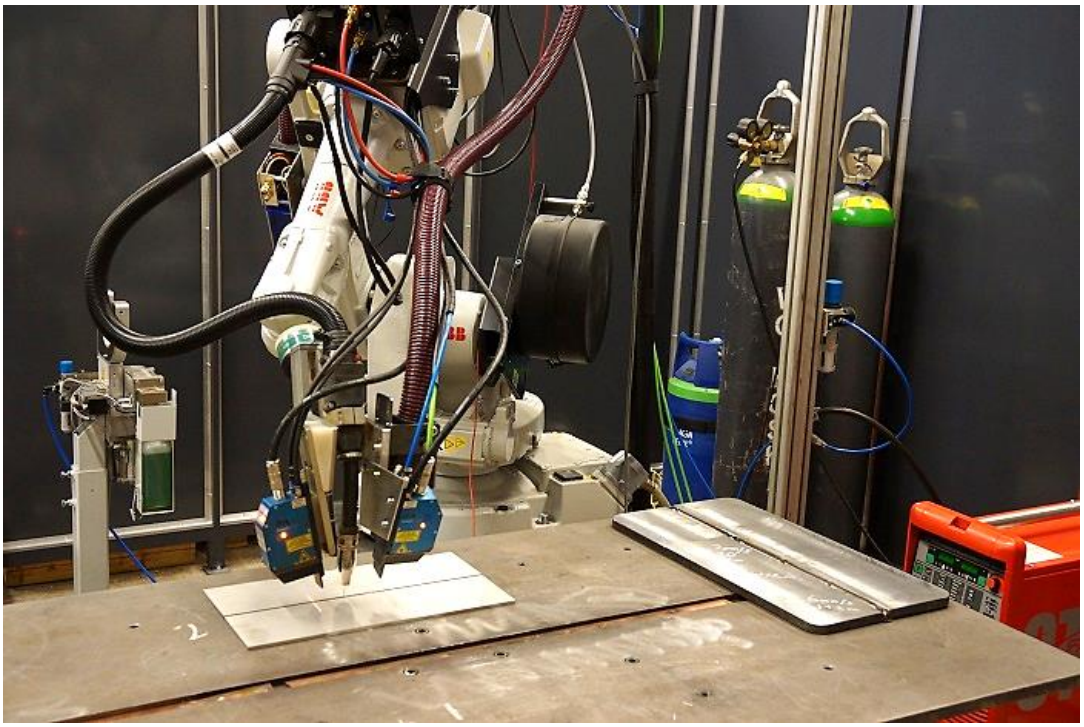

Figure 18. Adaptive welding station at Lappeenranta University of Technology.

The adaptive welding station was built around an industrial robot. The sensor set up and the adaptive welding head are shown in figure 19. The sensors around the torch take common welding orientations, such as butt joint and fillet joint are still usable.

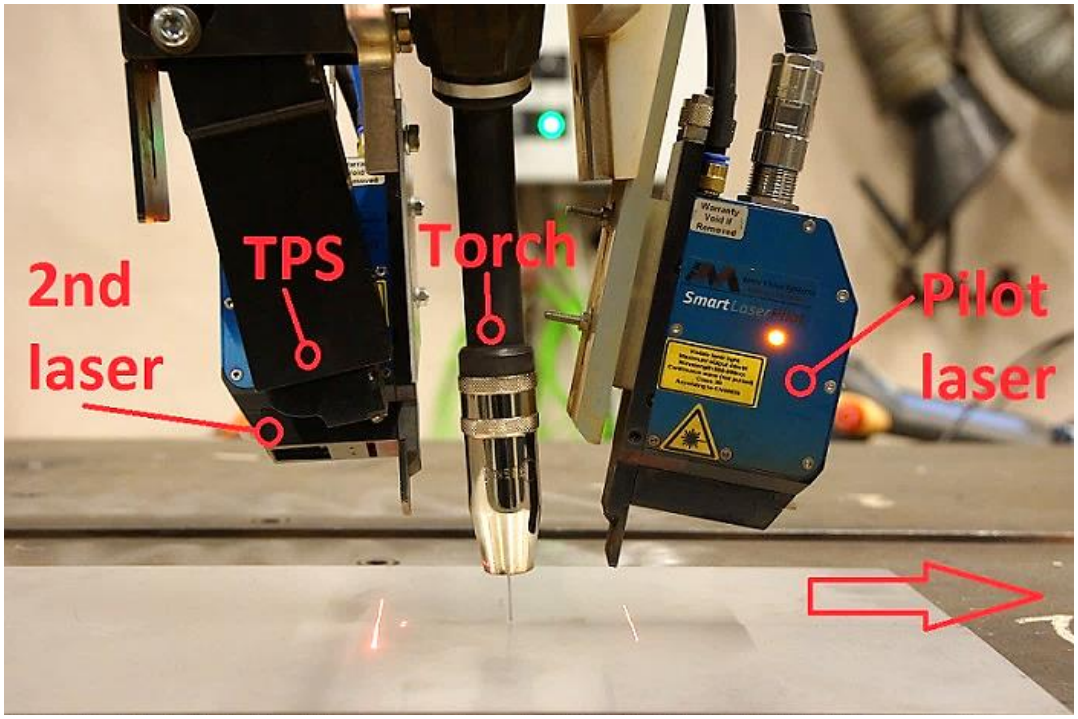

Figure 19. Adaptive welding head, including two laser sensors and TPS 34 mm behind the tip of the electrode wire. The arrow indicates travel direction.

The pilot laser in front of the welding torch finds and tracks the path as well as measures the groove geometry. ThermoProfilScanner behind the torch measures the thermography of the solidified, but still glowing weld. The second laser scanner is dedicated to measuring bead height. ThermoProfilScanner is based on measuring electromagnetic emissions in NIR band, emitted from hot weld surface. Both laser scanners are based on laser triangulation, typically used in laser tracking applications. All three sensors in the welding head send their data to a master computer.

6.1.1 Materials and test specimens

Since welding experiments have multiple variables, the results will be complex to analyse, unless essential parameters are identified. However, a neural network can solve this kind of problems, even though unimportant teaching parameters might cause noise and decrease the performance of the generated model. This issue led to the consideration that the most reasonable procedure to accomplish the experiments would be welding test specimens using constant process parameters while the root opening varies. The idea of the procedure was to achieve experiments that would include different penetration values, reducing the number of experiments and making comparison easier.

Experiments were carried out by butt welding machined V-grooves, without backing. The material used is S355K2 steel. Groove geometry, dimensions, and variables are shown in figure 20.

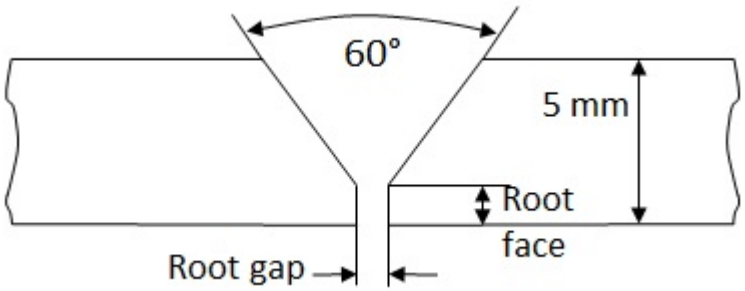

Figure 20. Groove cross-section geometry, dimensions and variables.

The experiments were performed by welding plates that have an opening root gap as illustrated in figure 21. Both step by step and linearly opening root gaps were tested. In addition, a few experiments were performed by welding plates that have a correspondingly decreasing root gap.

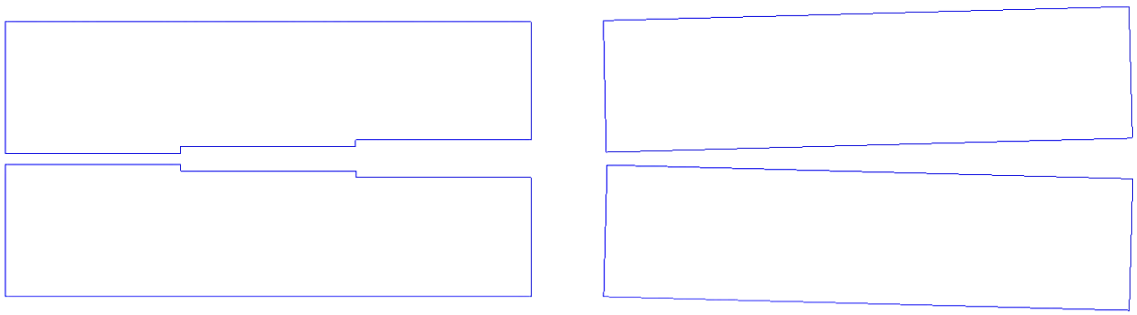

Figure 21. Illustrative sketches of the root openings of the test specimens.

The length of the test specimens was 400 mm, which allowed taking multiple specimens for macroscopic examination from one pair of workpieces.

6.1.2 Fixed process parameters

Fixed process parameters are presented in table 3. The constant welding parameters used are considered standard procedure for the MAG welding application studied.

Table 3. Constant welding parameters used in the experiments.

Description	Values
Material	S355K2
Plate thickness	5 mm
Groove angle	60°
Shield gas & flow rate	Ar + 12% CO_2, 17 l/min
Welding electrode	Esab OK Autrod 12.51, ⌀ 1 mm
Contact tip to work distance (CTWD)	18 mm

6.2 Welding of test specimens

The test specimens were tack welded and the root height and root face were measured before welding. To avoid distortion, the test specimens were clamped to the positioner table.

6.2.1 Procedure

The range of used process parameters is shown in table 4. Used parameter range was defined at the preliminary testing stage. It was found that even small adjustments had great effects on resulted weld attributes.

Table 4. Variable welding parameters and the identification of weld specimens.

Identification	Values
Gx.xHy.yWzz.zVqq.q (ArcL±pp)	
G = Root gap	0…1.5 mm
H = Root face height	0, 1, 2 mm
W = Electrode wire feed rate	9…10 m/min
V = Travel speed	6…7 mm/s
ArcL = Arc length (voltage) correction	0… +10 %
E.g. G1.0H2W10.0V7.0 ArcL+10	

To decrease the amount of experiments, the varied process parameters were altered by at least 10 % at a time. The welds specimens and the specimens for macroscopic evaluation were named with identifications represented in table 4.

6.2.2 Monitoring and data

Welding data was saved and extracted to an excel database by WeldQAS-system. The monitored parameters were IR thermography, current and voltage. Wire feed rate and gas flow were secondarily monitored to ensure a stable process. Fronius Trans Puls Synergic 5000 MAG welding power source was used in synergic mode.

6.3 Evaluation

Experiments were classified and evaluated on an Excel sheet, used as a neural network teaching data set (appendices). Penetration depth and the most important weld geometry attributes were measured from scaled pictures of specimens for macroscopic examination. Thermography temperatures were measured by median maximum temperature values of 40 neighbouring samples, which means about 0.5 s and 5 mm tolerance of the exact specimen point in a weld.

6.4 Qualification

The classification of the weld quality was based on the commonly used ISO 5817 standard. Penetration depth and root geometry were the analysed weld attributes. The standard does not allow incomplete root penetration in the most demanding B quality level welds nor in C level welds. The standard allows short term shrinkages and concavities in the groove (max. 5 % of the plate thickness, but max. 0.5 mm). However, all shrinkages and concavities were considered as faults in the experiments. In addition, excess penetration is a fault as defined in the standard. The limit for excess penetration in B level weld is presented in equation upcoming equation:

$$h \leq 1\ mm + 0.1 \times b, but\ max.\ 3\ mm \qquad (5)$$

in which h and b are the height and width of the root reinforcement. (SFS-EN ISO 5817, 2014.)

The test specimens were qualified with a scale of 0 to 2 in which 0 means proper B quality level weld, 1 means almost faulty B level weld and 2 faulty, non B level weld (appendix 2). The quality based classification of welds with different parameters was used for verifying the TPS sensor feedback as well as a teaching data set for the neural network.

The neural network was tested to simulate correction of wire feed rate based on the TPS sensor data and root geometry. However, arc length (voltage) correction was also found to impact penetration considerably due to its significant effect on heat input as presented in figure 22.

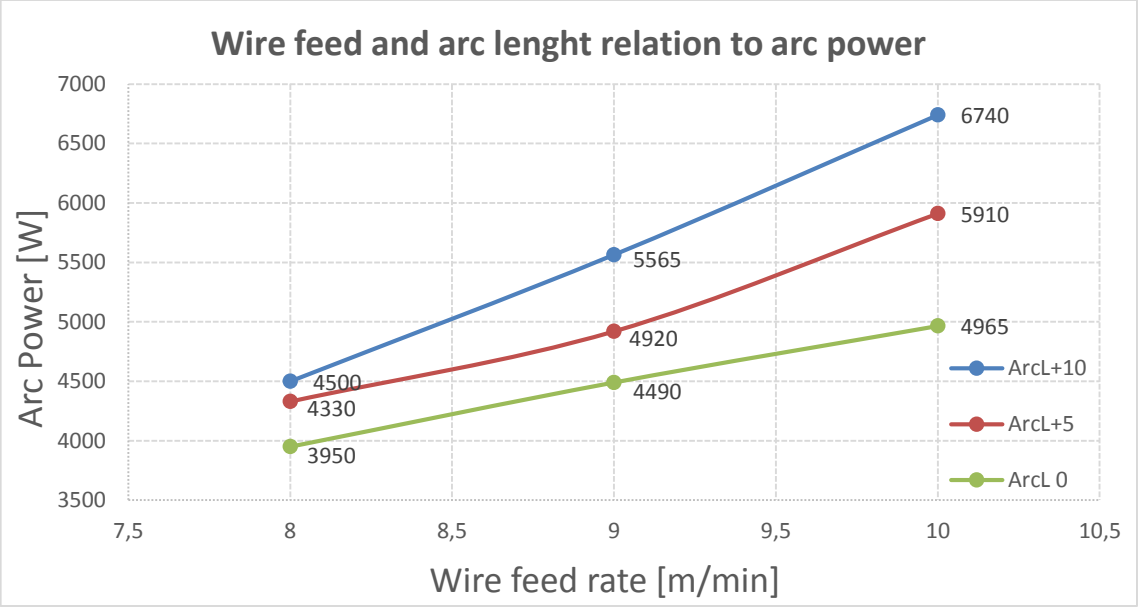

Figure 22. Wire feed and arc length relation to arc power.

However, this wire feed and arc length relation to arc power depend on the specific synergy curves of the used power supply. In addition, at least travel speed and groove filling require a closed loop control to be developed as a follow-up for this study.

7 RESULTS AND DISCUSSION

The experimental procedure was successful and it provided answers to the research questions. The infrared sensor and neural network both showed potential to evaluate the full penetration in MAG welding.

7.1 Accuracy of infrared thermography

The accuracy of near infrared photon detectors should in theory be about 1 °C which should be accurate enough for identifying crucial weld defects such as lack of penetration. Experiments in this study confirm this in practise, as can be seen in figure 23, where unmelted tack welds (2 and 3) can be seen as lower maximum temperatures and narrower width of thermal profile.

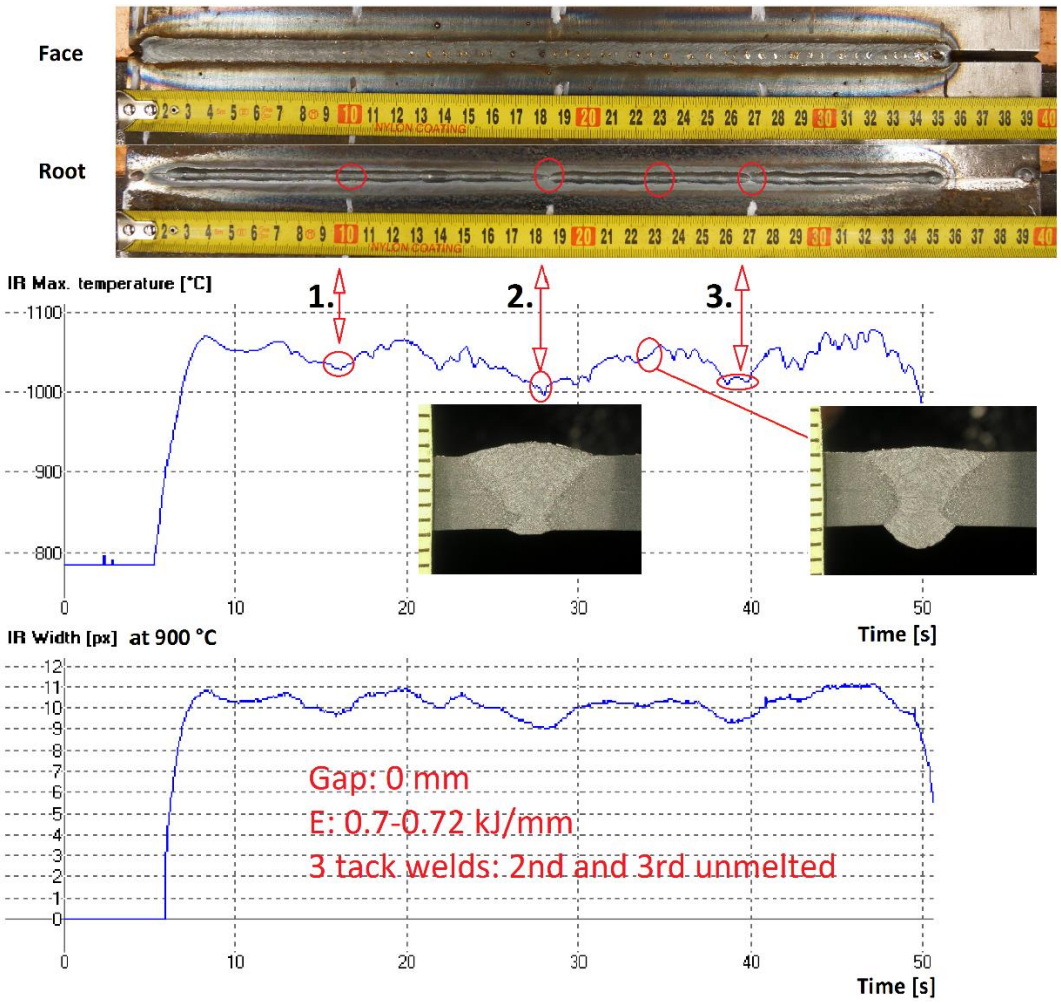

Figure 23. Unmelted tack welds vs. maximum IR temperature.

In this particular experiment, the tack welds were the only variable while process parameters were constant and air gap and root face were equal to 0 mm and 2 mm. Travel speed was 7 mm/s and wire feed rate was 10 m/min. The tack weld were welded to the root side by TIG welding equipment and grinded with an angle grinder. Tack welds were approximately 3–4 mm wide and 1–2 mm high. At the locations of the unmelted tack welds, the maximum temperatures are equal to 1000–1015 °C while elsewhere the maximum temperatures was significantly higher, equal to about 1050 °C. An interesting point is that the maximum IR temperature seems to indicate that the lack of penetration is longer than it actually is.

7.2 Thermal profile as a penetration control signal

The maximum IR temperature was found to have a relation to penetration as shown in figure 24. In this experiment, the welding parameters were constant except for the root gap which was increasing step by step. Travel speed, wire feed rate and arc length correction are equal to 6 mm/s, 9 m/min and +10 units. A hotter maximum temperature indicates a deeper weld penetration and correspondingly a colder maximum temperature indicates a shallower weld penetration. At the locations of specimens for macroscopic examination (1, 2 and 3), the maximum temperatures were equal to 1078 °C, 1126 °C and 1152 °C. The width of a thermal profile has a correlation to penetration as well, even though it does not have as much dynamic range as the maximum temperature with the studied sensor type. Previously, the maximum IR temperature and IR width have been proposed as penetration control signals by Nagarajan et al. (1989), Chen et al. (1990), and Chokkalingham et al. (2012). The sensor measurement distance was causing a measurement delay of 5–6 s, depending on the used welding speed. Even though arc welding seems to generate waving to thermal profiles possibly due to its short circuit based characteristics, there is still enough measurement range to identify the level of penetration.

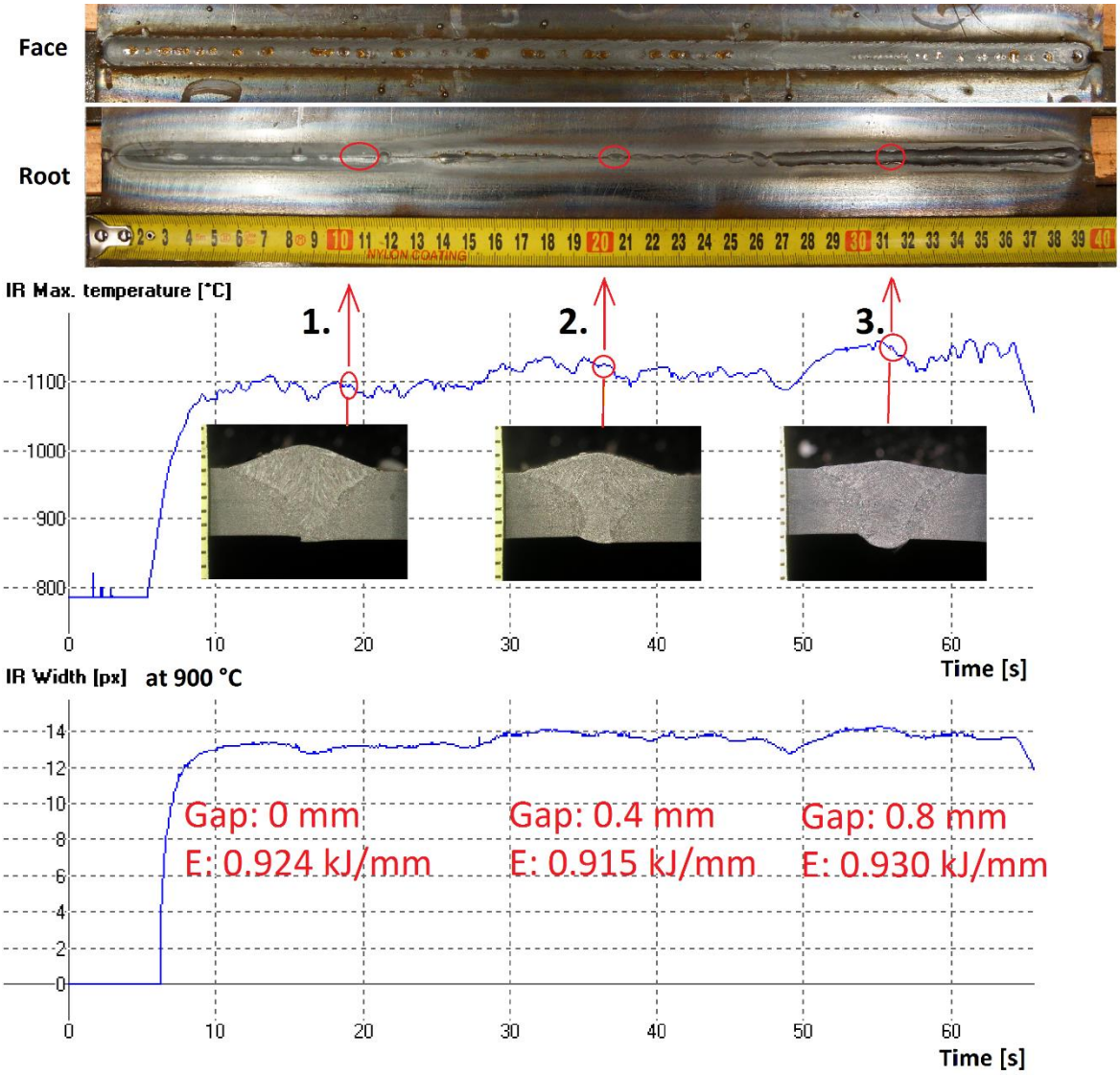

Figure 24. Penetration vs. maximum IR temperature.

7.3 Neural approach of weld penetration

Based on the experimental samples (appendices), a Levenberg-Marquard backpropagation neural network was created using MATLAB-software. The neural network (figure 25) has 3 input variables, maximum IR temperature (T_{max}), wire feed rate/travel speed ratio (W/V) and welding energy (E). These inputs are calculated in the hidden layers, which consist of 12 nodes. The output was the amount of wire feed correction required to obtain an acceptable weld. The teaching, testing and validation were made by randomly chosen samples. The distribution of samples was 60 % for teaching, 20 % for testing and another 20 % for validation.

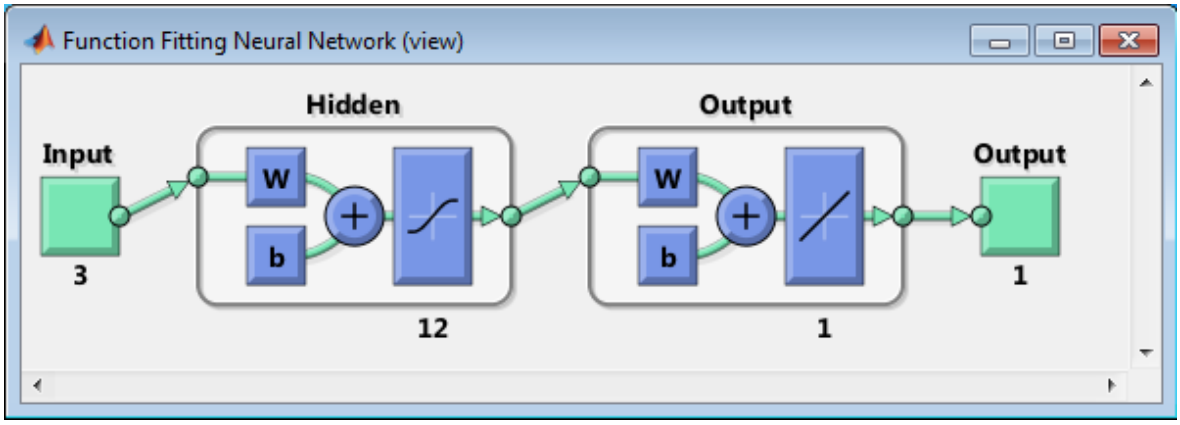

Figure 25. The basic structure of the neural network, where W is weight and b is bias.

During the first runs, the neural network performed with an average reliability of about 70 % with 39 randomly chosen teaching, testing and validation samples. The reliability of the neural network could be further improved to about 80 % by feeding more samples as presented in figure 26. The mean squared error (MSE) and the root mean squared error (RMSE) of the neural network fitting were equal to 0.114 and 0.338.

Some previous studies such as Chokkalingham et al. (2012) and Chandrasekhar et al. (2015) have achieved better results, however, they had twice the amount of teaching samples and more input parameters. In addition, in this study, the accuracy of the neural network could be improved by teaching more samples.

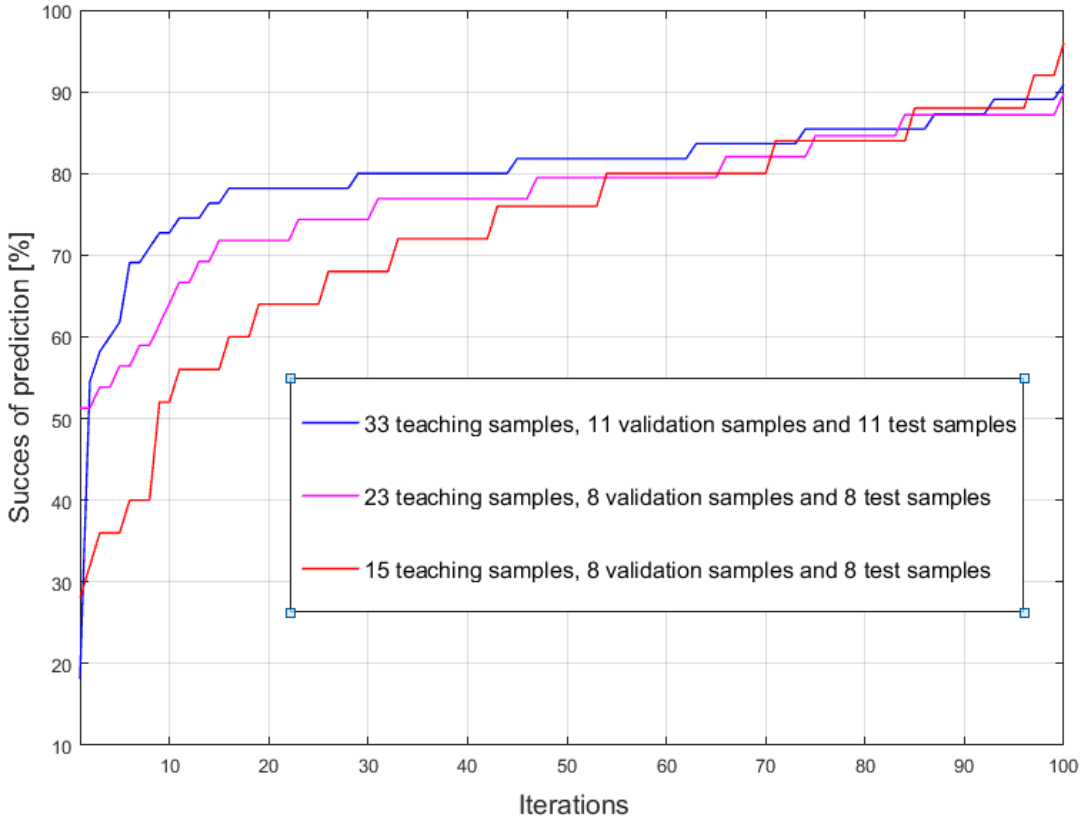

Figure 26. Success of the predictions tested with three different data sizes. In this case, an iteration means a full neural network teaching loop.

The logic of the neural network decision making principles was considered with known relations and causations, presented in figure 27. As it can be seen, there are two clusters linked together with arc energy (E) and travel speed (V). Thereby, the neural network is considered to model the right phenomenon.

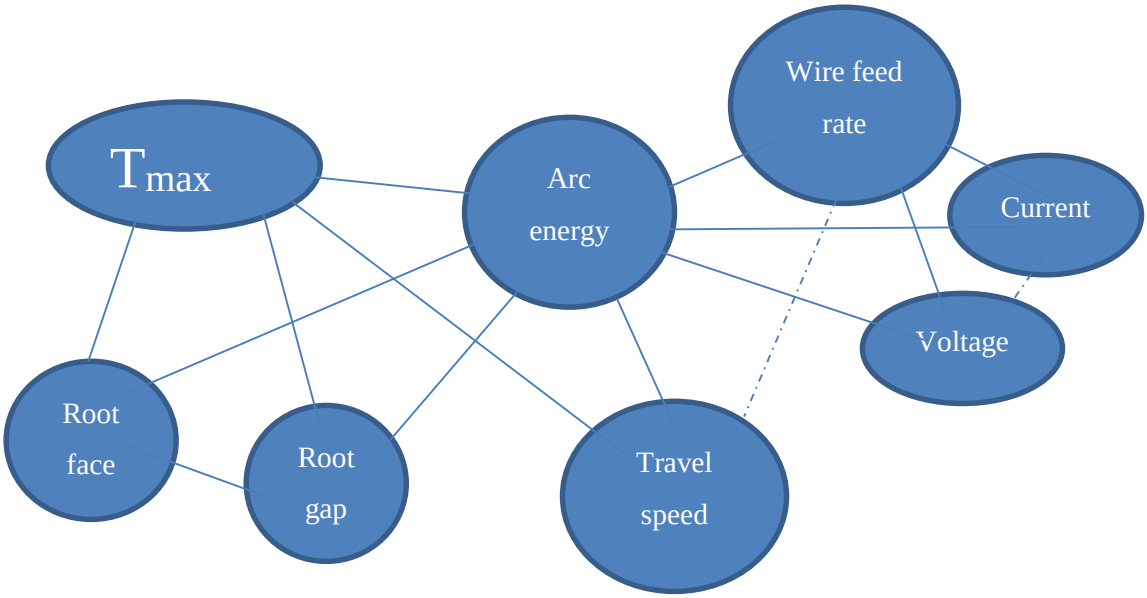

Figure 27. Known relations and causations of the maximum IR temperature (T_{max}) and the other process variables.

It is interesting that the neural network returned good results, even if groove geometry variables were excluded. Hence, it can be considered that maximum IR temperature (T_{max}) reveals the amount of penetration using only arc energy (E) and wire feed rate/travel speed ratio (W/V). Considering the accuracy of the neural network, it also indicates that the maximum IR temperature is an efficient signal for penetration control. The performance of the taught neural network in controlling the actual welding process will be studied in practise as a follow-up for this study.

ThermoProfilScanner has benefits compared to standard IR cameras, such as good accuracy, attachability to robot welding heads, less expensive price, good protection and small size. Though it still limits the reachability of the welding robot. For monitoring the penetration, the TPS needs to be coupled with current and voltage sensors as well as travel speed, because the measured maximum temperature also depends on the heat input. In addition, measuring the groove geometry before welding, for example by a laser sensor, has benefits in predicting the obtained penetration and groove filling.

8 CONCLUSIONS AND SUMMARY

An infrared thermography sensor and a neural network was studied as a full penetration control approach in gas metal arc welding. Experiments were performed by butt welding of S355 steel with V-grooves and without backing. During the experiments, the infrared thermography data and the other weld attributes were classified to a database which was used for verifying the infrared thermography sensor feedback as well as a teaching data set for the neural network. Based on literature review of the topic and executed experiments, the following conclusions can be stated:

Adaptive welding has been studied extensively, including various welding process control approaches. However, in the industry, adaptive welding is still not at the highest possible level. There is still a lot of need to develop more efficient adaptive welding systems.

Infrared thermography has shown potential in the estimation of weld penetration. Based on the experiments, the maximum temperature and the width of the temperature distribution were proved to correlate to the amount of weld penetration. Near infrared band is tolerant to emission variation of the measured object and suitable for measuring temperatures between approximately 500–1500 ºC. Photon detectors have an accuracy of approximately 1 ºC, which is more than enough for estimating the weld penetration. Based on the carried out experiments and previous studies found in literature, near infrared photon detectors are considered to be accurate enough to monitor full penetration.

The studied neural network showed potential as a penetration control approach. The neural network was performing well in the simulation of penetration estimation and wire feed rate correction considering that the teaching, validation and testing data included 55 samples. However, the neural network needs further development and improvement as a follow-up for this study. The thermography signal needs to be coupled with current and voltage sensors, because the measured temperature depends on heat input as well. The studied NIR line thermography sensor provides less information than actual NIR cameras. However, it is smaller, less expensive and still able to give reliable feedback on the amount of penetration.

Currently the most used approaches to model characteristics of the welding process are neural networks, fuzzy logic or combinations of these, which do not require accurate physical modelling of the welding process. However, neural networks tend to require a lot of work with teaching and validation. Nevertheless, the development of self-learning intelligent systems and pre-processed heuristics have potential to solve these problems.

9 FURTHER STUDIES

The following topic ideas can be proposed for further studies based on the result of this study:

1. Testing real life welding cases with the proposed full penetration control by the application of infrared thermography and neural network.

2. Improving the performance of the neural network model.

3. Developing a control of travel speed and groove filling.

4. Testing different seam types and groove geometries, plate thicknesses and materials such as stainless steel.

5. Multi sensor integration experiments with laser sensors.

REFERENCES

Alfaro, S. C. A. 2011. Sensors for Quality Control in Welding. In: Prof. Wladislav Sudnik (Ed.). Arc Welding. InTech. Pp. 81–106.

Astarita, T. & Carlomagno, G. M. 2013. Infrared Thermography for Thermo-Fluid Dynamics. Springer-Verlag Berlin Heidelberg. 224 p.

Aviles-Viñas, J. F., Lopez-Juarez, I. & Rios-Cabrera, R. 2015. Acquisition of welding skills in industrial robots. Industrial Robot: An International Journal, vol. 42:2. Pp. 156–166.

Carlomagno, G. M. & Cardone, G. 2010. Infrared thermography for heat transfer measurements. Experiments in Fluids, vol.49:1. Pp. 1187–1218.

Carrino, L., Natale, U., Nele, L., Sabatini, M.L. & Sorrentino, L. 2007. A neuro-fuzzy approach for increasing productivity in gas metal arc welding processes. International Journal of Advanced Manufacturing Technology, Vol. 32. Pp. 459–467.

Chen, W. H. & Chin, B. A. 1990. Monitoring Joint Penetration Using Infrared Sensing Techniques. Welding Journal, Vol. 69. Pp. 181–185.

Chen, S. B. 2015. On Intelligentized Welding Manufacturing. Robotic Welding, Intelligence and Automation, Advances in Intelligent Systems and Computing. Springer Switzerland. 32 p.

Chen, S. B. & Lv, N. 2014. Research evolution on intelligentized technologies for arc welding process. Journal of Manufacturing Processes, Vol. 16:1. Pp. 109–122.

Chen, X. Q., Luo, H. & Lin, W. J. 2007. Integrated Weld Quality Control System Based on Laser Strobe Vision. In: T.J. Tarn et al. (Eds.). Robot, Weld, Intelligence, & Automation. LNCIS. Springer-Verlag Berlin Heidelberg. Pp. 257–266.

Chandrasekhar, N., Vasudevan, M., Bhaduri, A. K. & Jayakumar, T. 2015. Intelligent modeling for estimating weld bead with and depth of penetration from infra-red thermal images of the weld pool. Journal of Intelligent Manufacturing, Vol. 26. Pp. 59–71.

Chokkalingham, S., Chandrasekhar, N. & Vasudevan, M. 2012. Predicting the depth of penetration and weld bead width from the infra red thermal image of the weld pool using artificial neural network modeling. Journal of Intelligent Manufacturing, Vol. 23:5. Pp. 1995–2001.

Cornu, J. 1988. Advanced welding systems. Welding Automation Vol. 2 Consumable electrode processes. IFS Publications Ltd, UK. 301 p.

Dinham, M. & Fang, G. 2013. Autonymous weld seam identification and localisation using eye-in-hand stereo vision for robotic arc welding. Robotics and Computer-Integrated Manufacturing, vol. 29. Pp. 288–301.

Einerson, J. C., Smartt, H. B., Johnson, J. A., Taylor, P. L. & Moore, K. L. 1992. Development of an intelligent system for cooling rate and fill control in GMAW. Proceedings of the 3rd International Conference on Trend in Welding Research, Washington, D.C., USA. Pp. 853–857.

Garašić, I. Kožuh, Z. & Remenar, M. 2015. Sensors and their classification in the fusion welding technology. Technical Gazette, Vol. 22:4. Pp. 1069–1074.

Ghanty, P., Vasudevan, M., Mukherjee, D. P., Pal, N. R., Chandrasekhar, N., Maduraimuthu, V., Bhaduri, A. K., Barat, P. & Raj, B. 2008. Artificial neural network approach for estimating weld bead width and depth of penetration from infrared thermal images of weld pool. Science and Technology of Welding and Joining, Vol. 13:4. Pp. 395–401.

Gruner, K. 2003. Princibles of Non-Contact Temperature Measurement [online]. Raytek GmbH. [Referred 6.1.2016]. 29 p. Available: http://support.fluke.com/raytek-sales/Download/Asset/IR_THEORY_55514_ENG_REVB_LR.PDF

Herman, K. Spong, N. & Lylynoja, A. 2004. Autonymous Manufacture of Large Steel Fabrications EC Contract: G1RD-CT-2000-00461 'NOMAD'. Proceedings of 35th International Symposium on Robotics, 23–26. March, Paris.

Heston, Tim. 2005. The Adaptability of Welding. Fabricating & Metalworking, Nov/Dec 2005; 4, 10; ProQuest. Pp. 41–45.

Hopko, S. N. Ume, I. C. & Erdahl, D. S. 2002. Development of a Flexible Laser Ultrasonic Probe. Journal of Manufacturing and Engineering, Vol. 124. Pp. 351–357.

HKS-Prozesstechnik. 2016a. ThermoProfilScanner [online]. [Referred 6.1.2016]. Available: http://www.hks-prozesstechnik.de/en/products/thermoprofilscanner/

HKS-Prozesstechnik. 2016b. ThermoProfilScanner [online]. [Referred 6.1.2016]. Available: http://www.hks-prozesstechnik.de/fileadmin/uploads/Downloads/flyer_tps_engl.pdf

HKS-Prozesstechnik. 2016c. WeldAnalyst [online]. [Referred 6.1.2016]. Available: http://www.hks-prozesstechnik.de/en/products/weldanalyst/

Hägale, M., Nilsson, K. & Pires, J. N. 2008. Industrial Robotics. In: Siciliano, B. & Khatib, O. (Eds.). Springer Handbook of Robotics. Springer-Verlag Berlin Heidelberg. Pp. 963-986.

Ithurralde, G., Simonet, D., Choffy, J.-P. & Bernard, L. 2000. NDT Approach and multi-sensors tools for the Inspection of aeronautics Welds. 15th World conference on non-destructive testing, Brescia.

Jang, J.-S. R., Sun, C.-T. & Mizutani, E. 1997. Neuro-Fuzzy and Soft Computing: A Computational Approach to Learning and Machine Intelligence. Upper Saddle River (NJ): Prentice Hall, cop. 614 p.

Juneghani, B. & Noruk, J. 2009. Keeping welding costs from spiraling out of control [online]. [Referred 16.12.2015]. Available: http://www.thefabricator.com/article/automationrobotics/keeping-welding--costs-from-spiraling--out-of-control

Köhler, T. 2015. Der ThermoProfilScanner in der Entwicklung und seine gegenwärtigen Eigenschaften und Formen zur Erfassung von Wärmefeldern in stark verschmutzten Umgebungen. HKS-Prozesstechnik GmbH. 10./11. Juni 2015. 24 p.

Köhler, T. 2016. ThermoProfilScanner - Technical data. HKS-Prozesstechnik GmbH. 17.2.2016. 1 p.

Lv, N., Zhong, J., Chen, H. & Lin, T. 2014. Real-time control of welding penetration during robotic GTAW dynamic process by audio sensing of arc length. The International Journal of Advanced Manufacturing Technology, Vol. 74. Pp. 235–249.

Meta Vision Systems, 2012. SLS-050 Preliminary Data Sheet [online]. Uploaded 04.2012. [Referred 17.11.2015]. Available: http://www.metamak.com.tr/wp-content/uploads/2012/04/MetaVision-SLS-Sensor-Datasheet.pdf

Meta Vision Systems, 2014. SLPi, Meta Laser Vision System for Robotic Welding [online]. Updated 28.1.2014. [Referred 17.11.2015]. Available: http://www.meta-mvs.com/QXBKN2146662

Mortimer, J. 2006. Jaguar uses adaptive MIG welding to join C-pillars to an aluminium roof section in a new sports car. Sensor Review, Vol. 26:4. Pp. 272–276.

Nagarajan, S., Chen, W. H. & Chin, B. A. 1989. Infrared Sensing for Adaptive Arc Welding. Welding Journal, vol. 68. Pp. 462–466.

Nagesh, D. S. & Datta, G. L. 2002. Prediction of weld bead geometry and penetration in shielded metal-arc welding using artificial neural networks. Journal of Materials Processing Technology, vol. 123:2. Pp. 303–312.

Naidu, D. S., Ozcelik, S. & Moore, K. L. 2003. Modeling, Sensing and Control of Gas Metal Arc Welding. First edition. Elsevier Science Ltd, Kidlington. 372 p.

Olson, D. L., Siewert, T. A., Liu, S. & Edwards, G. R. 1993. ASM Handbook, Volume 6: Welding, Brazing and Soldering. 10th edition. ASM International. 2872 p.

Pal, K., Bhattacharya S. & Pal, S. K. 2009. Prediction of metal deposition from arc sound and temperature signatures in pulsed MIG welding. The International Journal of Advanced Manufacturing Technology, Vol. 45. Pp. 1113–1130.

Pashkevich, A. 2009. Welding Automation. In: Nof, S. Y. (Ed.). Springer Handbook of Automation. Springer-Verlag Berlin Heidelberg. Pp. 1027–1040.

Pemamek. 2015. WeldControl 500 Adaptive [online]. [Referred 30.11.2015]. Available: http://www.pemamek.com/automated-welding/pema-weldcontrol/weldcontrol-500-adaptive

Pires, J. N., Loureiro, A. & Bölmsjo, G. 2006. Welding Robots: technology, system issues and applications. Springer-Verlag London Limited. 180 p.

Planck, M. 1900. Über eine Verbesserung der Wien'schen Spectralgleichung. Verhandlungen der Deutschen Physikalischen Gesellschaft 2. Verlag von Johann Ambrosius Barth, Leipzig. Pp. 202–204.

Schauder, V., Köhler, T., Wenzl, B., Prasek, & M. Schmitt, M. 2013. Thermal Weld Seam Inspection in Pipe Production Lines. IIW International Conference on "Automation in Welding" 16th/17th September, 2013. Essen, Germany.

Schiewe, C. & Schindler, K. 2013. The influence of the emissivity on the non-contact temperature measurement [online]. DIAS Infrared Systems. [Referred 14.2.2016]. 3 p. Available: http://www.dias-infrared.com/wp-content/uploads/sites/2/2013/03/Influence_Of_Emissivity.pdf

SCOPUS. 2016. Tools for analyzing scientific articles [online]. [Referred 14.2.2016]. Available: https://www.scopus.com/term/analyzer.uri?sid=09D6F01A8E652CB44BBA2E86EACF0811.CnvicAmOODVwpVrjSeqQ%3a20&origin=resultslist&src=s&s=TITLE-ABS-KEY%28adaptive+OR+intelligent+OR+automated+AND+welding%29&sort=plf-f&sdt=b&sot=b&sl=63&count=3982&analyzeResults=Analyze+results&txGid=0

SFS 3052. 1995. Welding terminology. The Finnish Standard Association. Approved on 25th September 1995. 122 p.

SFS-EN ISO 5817. 2014. Welding. Fusion-welded joints in steel, nickel, titanium and their alloys (beam welding excluded) - Quality levels for imperfections. The Finnish Standard Association. Approved on 31st March 2014. 61 p.

Smartt, H. B. & Einerson, C. J. 1993. A Model for Heat and Mass Input Control in GMAW. Welding Journal, May 1993. Pp. 217–229.

Tay, K. M. & Butler, C. 1997. Modelling and optimatizing of a MIG welding process – A case study using experimental designs and neural networks. Quality and Reliability Engineering International, Vol. 13. Pp. 61–70.

Thermatool. 2016. SeamScan [online]. [Referred 14.2.2016]. Available: http://thermatool.com/blog/products/seamscan/

Wang, Z. Zhang, Y. & Wu, L. 2012. Adaptive interval model control of weld pool surface in pulsed gas metal arc welding. Automatica, Vol. 48:1. Pp. 233–238.

Xiong, J., Zhang, G., Hu, J. & Li, Y. 2013a. Forecasting process parameters for GMAW-based rapid manufacturing using closed-loop iteration based on neural network. International Journal of Advanced Manufacturing Technology, Vol. 69. Pp. 743–745.

Xiong, J., Zhang, G., Hu, J. & Li, Y. 2013b. Vision-sensing and bead width control of a single-bead multi-layer part: material and energy savings in GMAW-based rapid manufacturing. Journal of Cleaner Production, Vol. 41. Pp. 82–88.

You, D. Y. Gao, X. D. & Katayama, S. 2014 Review of laser welding monitoring. Science and Technology of Welding and Joining, Vol. 19:3. Pp. 181–201.

Zahran, O.Hasban, H. El-Kordy, M. & El-Samie, F. E. 2013. Automatic weld defect identification from radiographic images. NDT & E International, Vol. 57. Pp. 26–35.

Welding parameters and identifications.

Specimen number (#), groove geometry and welding parameters							
#	Groove	G	H	Parameters	W	V	ArcL
		mm	mm		m/min	mm/s	
1	G0.5H1	0.5	1	W9V7 ArcL +10	9	7	+10
2	G0.9H1	0.9	1	W9V7 ArcL +10	9	7	+10
3	G0.6H1	0.6	1	W9V7 ArcL +10	9	7	+10
4	G0H1	0	1	W9V7 ArcL +10	9	7	+10
5	G0H1	0	1	W9V7 ArcL +10	9	7	+10
6	G0.6H1	0.6	1	W9V7 ArcL +10	9	7	+10
7	G1.0H1	1	1	W9V7 ArcL +10	9	7	+10
8	G0H2	0	2	W9V6 ArcL +10	9	6	+10
9	G0.4H2	0.4	2	W9V6 ArcL +10	9	6	+10
10	G0.8H2	0.8	2	W9V6 ArcL +10	9	6	+10
11	G0.5H2	0.5	2	W9V6	9	6	0
12	G0.7H2	0.7	2	W9V6	9	6	0
13	G0.9H2	0.9	2	W9V6	9	6	0
14	G1.0H2	1	2	W9V6	9	6	0
18	G0.2H2	0.2	2	W10V7 ArcL +10	10	7	+10
19	G0.7H2	0.7	2	W10V7 ArcL +10	10	7	+10
20	G0.9H2	0.9	2	W10V7 ArcL +10	10	7	+10
21	G0.2H0	0.2	0	W10V7	10	7	0
22	G0.2H0	0.2	0	W10V7	10	7	0
23	G0.8H1	0.8	1	W9V6 ArcL +10	9	6	+10
24	G0.4H1	0.4	1	W9V6 ArcL +10	9	6	+10
25	G1.1H1	1.1	1	W10V7 ArcL +10	10	7	+10
26	G0.8H1	0.8	1	W10V7 ArcL +10	10	7	+10
27	G0.6H1	0.6	1	W10V7 ArcL +10	10	7	+10
28	G0.9H2	0.9	2	W10V7	10	7	0
29	G0.5H2	0.5	2	W10V7	10	7	0
30	G0H2	0	2	W10V7	10	7	0
31	G1.1H2	1.1	2	W9V7 ArcL +10	9	7	+10
32	G0.7H2	0.7	2	W9V7 ArcL +10	9	7	+10
33	G0H2	0	2	W9V7 ArcL +10	9	7	+10
34	G0.4H0	0.4	0	W9V6	9	6	0
35	G0.7H0	0.7	0	W9V6	9	6	0
36	G0H0	0	0	W9V7	9	7	0
37	G0.8H0	0.8	0	W9V7	9	7	0
38	G0.5H2	0.5	2	W9V7	9	7	0
39	G0.7H2	0.7	2	W9V7	9	7	0
40	G0.2H2	0.2	2	W9V7	9	7	0

Welding parameters and identifications.

Specimen number (#), groove geometry and welding parameters							
#	Groove	G	H	Parameters	W	V	ArcL
		mm	mm		m/min	mm/s	
41	G0H2	0	2	W9V7	9	7	0
42	G0H2	0	2	W9V7 ArcL +10	9	7	+10
43	G0H2	0	2	W9V6	9	6	0
44	G0.7H2	0.7	2	W9V6 ArcL +10	9	6	+10
45	G0H2	0	2	W9V6 ArcL +10	9	6	+10
46	G0.7H2	0.7	2	W9V6	9	6	0
47	G0.5H2	0.5	2	W9V6 ArcL +10	9	6	+10
48	G1H2	1	2	W9V6 ArcL +10	9	6	+10
49	G0.2H2	0.2	2	W10V7	10	7	0
51	G0H2	0	2	W10V7 ArcL +5	10	7	+5
52	G1H1	1	1	W10V8 ArcL +5	10	8	+5
53	G0.2H1	0.2	1	W9,5V7 ArcL +10	9.5	7	+10
57	G0.3H2	0.3	2	W9V7 ArcL +10	9	7	+10
58	G0.3H2	0.3	2	W9V7 ArcL +10	9	7	+10
62	G0.3H2	0.3	2	W9V7 ArcL +10	9	7	+10
66	G0.2H1	0.2	1	W9,5V7 ArcL +10	9.5	7	+10
70	G0.2H2	0.2	2	W9,5V7 ArcL +10	9.5	7	+10
74	G1H0	1	0	W9V7 ArcL +10	9	7	+10
75	G1,5H0	1	0	W9V7 ArcL +10	9	7	+10

Weld attributes and qualifications.

#	Root width	Root height		Quality	Tmax	E	Arc power
	mm	(- = lack of penetration) mm	Allowed root height	0 = OK, 1 = 'almost' and 2 = fault	(Median) °C	(Median) kJ/mm	W
1	4.9	1.4	2.0	0	1091.2	0.792	5544
2	5.3	1.5	2.1	0	1113	0.813	5688
3	3.7	0.3	1.7	0	1117	0.819	5739
4	1.8	0	1.4	1	1076.8	0.821	5746
5	5.4	1.2	2.1	0	1064.8	0.785	5496
6	5.1	1.4	2.0	0	1079.1	0.772	5406
7	5.5	1.4	2.1	0	1113	0.776	5430
8	0.0	-0.4	1.0	2	1077.8	0.924	5546
9	2.5	0.14	1.5	1	1126.3	0.915	5492
10	3.7	0.7	1.7	0	1151.5	0.930	5581
11	0.0	-1.1	1.0	2	948.9	0.731	4388
12	1.2	0	1.2	1	960.9	0.735	4411
13	2.7	0.5	1.5	0	977.3	0.753	4517
14	3.6	1	1.7	0	971.3	0.711	4266
18	5.8	2.5	2.2	2	1211.2	0.959	6717
19	5.0	1.9	2.0	0	1253.6	0.959	6717
20	6.1	2.6	2.2	2	1234.3	0.959	6717
21	5.3	1.6	2.1	0	1052.6	0.721	5050
22	2.8	0	1.6	2	1014.6	0.697	4882
23	3.8	0.3	1.8	0	1161.5	0.931	5588
24	3.4	0.3	1.7	0	1128.6	0.941	5647
25	6.3	2.0	2.3	0	1287.9	0.956	6691
26	5.4	1.6	2.1	0	1266.5	0.965	6754
27	3.8	0.3	1.8	0	1291.1	0.969	6780
28	4.9	1.5	2.0	0	1069.2	0.712	4983
29	1.7	0.2	1.3	1	989.1	0.712	4984
30	0.0	-0.7	1.0	2	956.9	0.704	4929
31	5.0	1.5	2.0	0	1127.4	0.805	5636
32	3.0	0.2	1.6	0	1119.7	0.809	5664
33	0.9	0	1.2	1	1070	0.808	5653
34	2.1	0.1	1.4	0	1024.3	0.740	4442
35	4.2	0.8	1.8	0	1023.1	0.758	4546
36	1.4	0.1	1.3	1	945.6	0.644	4506
37	5.0	1.3	2.0	0	989.2	0.649	4541
38	1.5	0.1	1.3	1	939.6	0.639	4479
39	0.2	-0.1	1.0	2	951.4	0.634	4439
40	0.0	-0.5	1.0	2	936.6	0.641	4485

APPENDIX II, 2

Weld attributes and qualifications.

#	Root width	Root height		Quality	Tmax	E	Arc power
	mm	(- = lack of penetration) mm	Allowed root height	0 = OK, 1 = 'almost' and 2 = fault	(Median) °C	(Median) kJ/mm	W
41	0.0	-1.4	1.0	2	882.6	0.623	4358
42	3.6	1.0	1.7	0	1092.5	0.864	6049
43	0.0	-1.7	1.0	2	955.9	0.726	4355
44	3.4	0.4	1.7	0	1121.8	0.931	5583
45	0.0	-1.4	1.0	2	1101.6	0.932	5594
46	2.9	0.2	1.6	0	951.3	0.725	4352
47	5.6	1.8	2.1	0	1122.5	0.917	5501
48	5.3	1.7	2.1	0	1123.7	0.925	5551
49	1.3	0.1	1.3	0	1006.3	0.738	5167
51	3.8	0.8	1.8	0	1130.1	0.883	6179
52	5.8	1.7	2.2	0	1134.9	0.783	6260
53	4.6	1.0	1.9	0	1166	0.901	6305
57	0.0	-1.0	1.0	2	1028.4	0.768	5377
58	0.0	-0.9	1.0	2	1028.2	0.783	5478
62	2.4	0.2	1.5	0	1026.9	0.783	5482
66	3.2	0.2	1.6	0	1128.6	0.873	6114
70	3.2	0.3	1.6	0	1127.5	0.875	6128
74	6.9	1.5	2.4	0	1125.3	0.784	5491
75	5.9	1.0	2.2	0	1124.8	0.792	5547